Sagittal crest morphology decoupled from relative bite performance in Pleistocene tapirs (Perissodactyla: Tapiridae)

Sagittal crest morphology decoupled from relative bite performance in Pleistocene tapirs (Perissodactyla: Tapiridae).

Running title: Tapir bite forces and sagittal crests.

Lisa Van Linden[1*], Kim Stoops[1], Larissa C. C. S. Dumbá[2], Mario A. Cozzuol[2], Jamie A. MacLaren[1,3*]

[1] Functional Morphology Lab, Department of Biology, Campus Drie Eiken, Universiteit Antwerpen, Universiteitsplein 1, 2610 Antwerpen, Belgium

[2] Departamento de Zoologia, Instituto de Ciências Biológicas, Universidade Federal de Minas Gerais, Avenida Antônio Carlos 6627, Belo Horizonte, 31270-901 Minas Gerais, Brazil

[3] Evolution & Diversity Dynamics Lab, Department of Geology, Université de Liège, Quartier Agora, Allée du six Août 14, 4000 Liège, Belgium

*corresponding authors

Corresponding Authors: Lisa Van Linden & Jamie A. MacLaren

Email Address: lisa.vanlinden@uantwerpen.be, jamie.maclaren@uantwerpen.be

Institutional Address:

University of Antwerp
Department of Biology
Universiteitsplein
Wilrijk, Antwerpen
2610 BELGIUM

Abstract

Bite force is often associated with specific morphological features, such as sagittal crests. The presence of a pronounced sagittal crest in some tapirs (Perissodactyla: Tapiridae) was recently shown to be negatively correlated with hard-object feeding, in contrast with similar cranial structures in carnivorans. The aim of this study was to investigate bite forces and sagittal crest heights across a wide range of modern and extinct tapirs and apply a comparative investigation to establish whether these features are correlated across a broad phylogenetic scope. We examined a sample of 71 specimens representing 15 tapir species (five extant, ten extinct) using the dry-skull method, linear measurements of cranial features, phylogenetic reconstruction, and comparative analyses. Tapirs were found to exhibit variation in bite force and sagittal crest height across their phylogeny and between different biogeographical realms, with high-crested morphologies occurring mostly in Neotropical species. The highest bite forces within tapirs appear to be driven by estimates for the masseter – pterygoid muscle complex, rather than predicted forces for the temporalis muscle. Our results demonstrate that relative sagittal crest height is poorly correlated with relative cranial bite force, suggesting high force application is not a driver for pronounced sagittal crests in this sample. The divergent biomechanical capabilities of different contemporaneous tapirids may have allowed multiple species to occupy overlapping territories and partition resources to avoid excess competition. Bite forces in tapirs peak in Pleistocene species, independent of body size, suggesting possible dietary shifts as a potential result of climatic changes during this epoch.

Keywords: Dry skull method – Herbivory – Niche partitioning – Mastication – Pleistocene – Biogeography

Graphical Abstract

We quantified bite force and sagittal crest height across modern and extinct tapirids using the dry-skull method. Our results demonstrate a poor correlation between relative sagittal crest height and bite force. Tapirs exhibit variation in bite force and sagittal crest height, with high-crested morphologies occurring mostly in Neotropical species. Bite forces peak in the Pleistocene, independent of body size, with contemporaneous tapirs displaying divergent biomechanical capabilities.

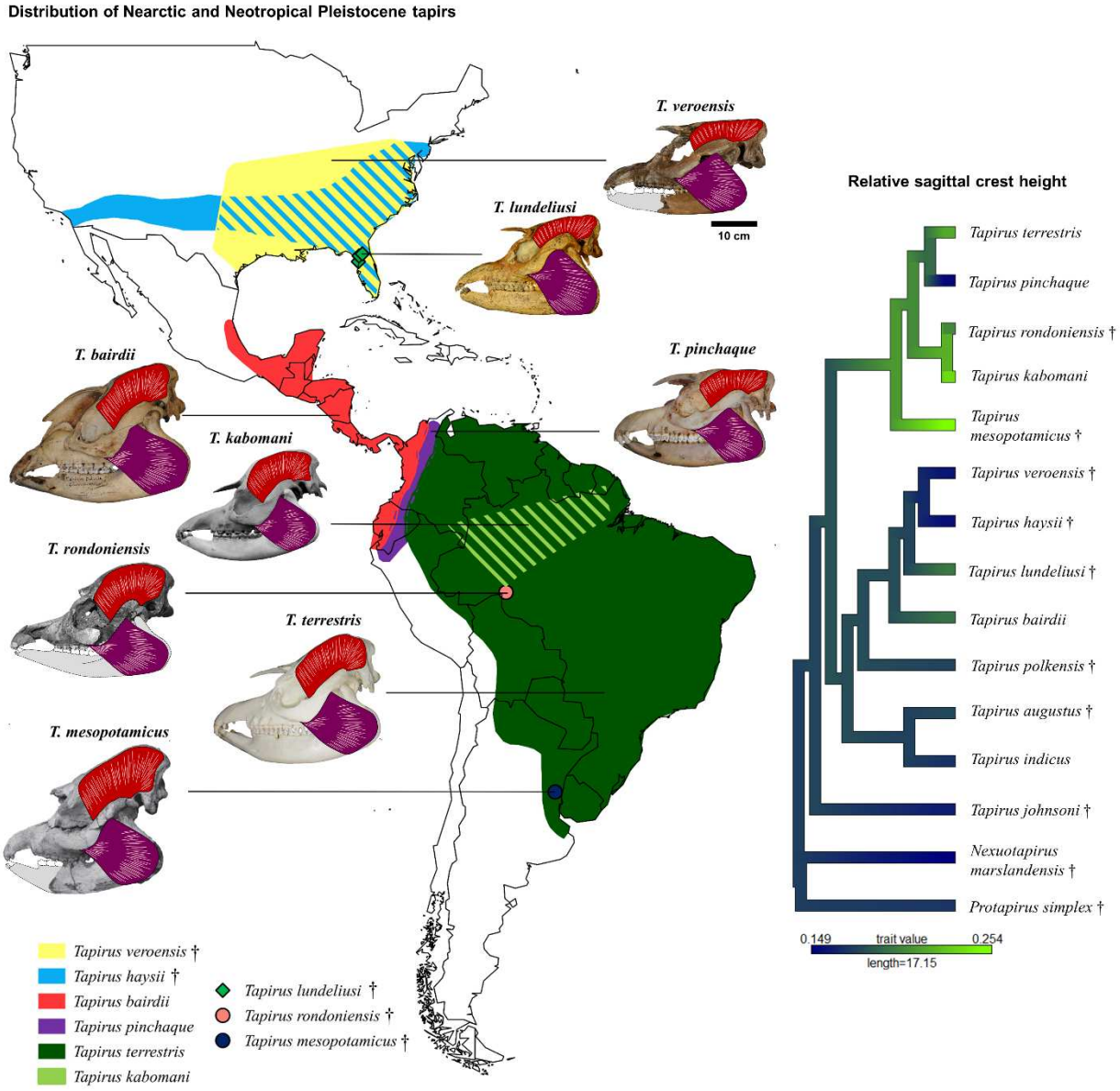

Introduction

Tapirs (Perissodactyla: Tapiridae) are large, odd-toed ungulate mammals that belong to the order Perissodactyla (odd-toed hooved mammals), together with equids and rhinoceroses. There are five extant tapir species (Cozzuol et al., 2013), all belonging to the family Tapiridae and the genus *Tapirus* Brünnich, 1772 (Table 1). This small number of extant tapir species represents only a small part of the rich fossil history of tapirids (Colbert, 2006; Holanda, 2006; Hulbert, 2010; Ji et al., 2015; Radinsky, 1966; Scherler et al., 2011). Modern tapirs are distributed around the Neotropics (Central and South America) and Southeast Asia (Holanda, 2006), although their range throughout the Cenozoic also included the Indo-Malayan and Nearctic up until the end-Pleistocene. Tapirs tend to inhabit dense tropical and sub-tropical forests, wooded grassland, and montane woodland biomes (DeSantis, 2011; Padilla and Dowler, 1994; Padilla et al., 2010). Most extinct species occurred in similar habitats, although some are known from more temperate regions, especially during the Plio-Pleistocene (Czaplewski et al., 2002; de Soler et al., 2012; Graham et al., 2019; MacLaren et al., 2018). Tapirs are primarily herbivorous (Koch et al., 1998; Kohn et al., 2005; MacFadden and Cerling, 1996), with their diets consisting mostly of foliage, fruits, seeds, and other plant material (Henry et al., 2000; Savage and Long, 1986). These components are known to be consumed to different degrees in different modern tapir species (DeSantis, 2011; Downer, 2001; Henry et al., 2000; Janzen, 1982; O'Farrill et al., 2013). Tapir skulls exhibit a great deal of variation in the attachment sites of the temporalis musculature, i.e., the sagittal crest (DeSantis et al., 2020; Dumbá et al., 2018; Hulbert et al., 2009); with no observed sexual dimorphism (Rojas et al., 2021). A good example of this variation is the different crest morphologies exhibited by extant tapirs (Figure 1). Within extant tapirs, sagittal crests can vary from a broad sagittal table (e.g., *T. bairdii* Gill, 1865; Figure 1a) to a narrow crest (e.g., *T. pinchaque* Roulin, 1829; Figure 1b); the relative height of the dorsal surface of the cranium from the toothrow can also greatly vary, from a relatively high skull (e.g., *T. terrestris* Linnaeus, 1758; Figure 1c) to a comparatively shallow skull (e.g., *T. indicus* Desmarest, 1819; Figure 1d).

A recent multidisciplinary study that used finite element analysis and dental microwear texture analysis suggested that the presence of a pronounced sagittal crest in tapirs is negatively correlated with feeding on hard objects (DeSantis et al., 2020), unlike the presence of similar cranial structures in carnivorans (Van Valkenburgh, 2007). The masticatory muscles consist of the temporalis muscle (*musculus temporalis*) and the masseter – pterygoid muscle complex (*m. masseter* + *m. pterygoideus*). A large sagittal crest allows for an expansion of the attachment area for the *m. temporalis* muscle, one of the principal jaw adductors (Van Valkenburgh, 2007). The presence of large sagittal crests (e.g., in *T. terrestris*,) was interpreted as being beneficial for the

continuous processing of tough and less nutritious vegetative matter (DeSantis et al., 2020), rather than conferring large forces for breaking open hard-shelled seeds or nuts (as seen in *T. indicus*, Campos-Arceiz et al., 2012).

Studies of bite force vary widely in methodology, and each methodology comes with its suite of limitations. For example, *in vivo* measurements of bite force provide direct estimations, but samples are often limited, and working alongside live animals can be dangerous (Davis et al., 2010; Herrel et al., 2008; Law and Mehta, 2019); biomechanical modeling with freshly dissected feeding apparatuses can be challenging due to the difficulty of obtaining deceased individuals of wild or rare animals (Davis et al., 2010; Gignac and Erickson, 2016; Hartstone-Rose et al., 2012; Santana et al., 2010). Many mammalogists estimate bite forces using models; the most frequently used is a two-dimensional picture-based technique known as the "dry skull method" (Thomason 1991). This method relies on estimated cross-sectional areas of the jaw adductor muscles from photographs of skulls (Law and Mehta, 2019; Thomason, 1991). Photographs can be easily obtained, as the skulls are often part of museum collections, and can thus be used to study large numbers of extant and extinct species to explore patterns of bite force through time or across large phylogenetic groups (e.g., Sakamoto et al., 2010; Snively et al., 2015; Wroe et al., 2005).

A comparative investigation of bite forces and sagittal crest heights across a large sample of modern and extinct tapirs may elucidate their functional relationship, providing new insights on bite force mechanics in herbivores and the relationship between morphology (sagittal crest height) and performance (bite force). We might expect potential force application across the Tapiridae to be negatively correlated with increased sagittal crest height, a working hypothesis supported by the recent study of DeSantis et al. (2020). More broadly, shifts in masticatory mechanics and potential bite force may in fact relate to the exploitation of different foodstuffs or biomes or may be phylogenetically linked. Exploring morphological/performance patterns across a broad phylogenetic scope may demonstrate historical constraints on the height of the sagittal crest or bite force application in this enigmatic ungulate clade. Here, we apply the dry-skull method to 15 species (five extant, ten extinct) of tapirids, calculating bite forces at multiple points along the upper toothrow. We compare bite forces across extinct and extant species, assessing the results with respect to sagittal crest height, phylogenetic relationships, and geographical ranges. We expect estimated bite forces to be highest in larger species with larger skulls; however, in relative terms, we anticipate lower bite forces relative to skull size in species with higher sagittal crests, in keeping with results from recent biomechanical modelling approaches (DeSantis et al., 2020). We also hypothesize that masticatory performance will be notably divergent between tapir species exploiting different biogeographical realms, with the associated differences in habitat acting as a

stronger selective pressure on morphology and performance than similarities due to phylogenetic affinity.

Methodology

Specimen Image Collection

To investigate masticatory mechanics and its relationship to sagittal crest size in tapirs, a sample of 71 specimens of modern and extinct tapir crania (15 species) was collected, accounting for 23% of all described tapirid species (Behrensmeyer and Turner, 2013) (Table 1). Most specimens were photographed first hand in lateral, dorsal, and palatal views, with additional specimens (mostly extinct) taken from publication figures (see Table S1 for the specimen list). Specimens were sought to have at least M2 erupted/erupting to minimize the influence of age. No sexual dimorphism has been found in tapir crania (Rojas et al., 2021), thus we do not account for this.

Skull Measurements

A series of measurements were recorded on scaled two-dimensional images of tapir skulls using ImageJ (Schindelin et al., 2012). Measurements were derived from the methods of Campbell and Santana (2017) and Thomason (1991) and adapted accordingly to fit herbivore skulls. Photographs were taken perpendicular to the maxillary toothrow (dorsal and ventral), rather than down the predicted line of temporalis (*musculus temporalis*) and/or masseter + pterygoid (*m. masseter* + *m. pterygoideus*) muscle action; this method was chosen to maximize specimens and species coverage, and incorporate images from publications (Figure 2). While not strictly representing the cross-sectional area and/or biological line-of-action of the muscles in question, measurements taken using these images enabled comparisons across a large range of species and specimens while retaining methodological consistency.

The following linear measurements were taken: cranium length (C_L), sagittal crest height (SC_H), moment arms (*mp* and *t*), and out-levers (O) (Figure 2). C_L was measured from the anterior-most point of the premaxilla to the occipital condyle. SC_H was measured from the posterior-most point of the zygomatic arch to the tallest point on the skull (with the toothrow held horizontal). *mp* represents the moment arm of the *m. masseter* + *m. pterygoideus* muscles, measured from the temporomandibular joint (TMJ) to the centroid of the *m. masseter* + *m. pterygoideus* muscle complex. *t* represents the moment arm of the temporalis muscle measured from the TMJ to the centroid of the *m. temporalis*. O_i represents the out-levers for each tooth measured from the TMJ to the posterior edge of the respective tooth (to ensure uniform measurements between all

observers). Measurements were taken three times (three observers) for all individuals and averaged. The out-levers were measured for the different tooth types, as they are each specialized for a certain function: the caniniform incisor, which is used for food manipulation (Milewski and Dierenfeld, 2013), and the premolars and molars which do the majority of the food processing during the chewing cycle (Engels and Schultz, 2019). The regular incisors were not used here because these are the grasping teeth with little manipulatory or masticatory functions in tapirs (Milewski and Dierenfeld, 2013).

In addition to these linear measurements, two muscle areas were calculated: *m. masseter* + *m. pterygoideus* muscle cross-sectional area (MP), measured from ventral view, bounded by the zygomatic arch and basicranium; and the *m. temporalis* muscle cross-sectional area (T), measured from dorsal view, bounded by the zygomatic arch and braincase. The area measurements of the muscles were used to estimate bite forces (see further), as it is assumed that the forces created are linearly correlated with the dimensions of the masseter and temporalis muscles combined with the moment arms, and that the forces are limited by the intrinsic strength of the mandible (avoiding mandible failure during maximal force application) (Currey, 2006; Demes, 1982; Thomason, 1991).

Bite Force Calculations

Dry Skull Bite Force

Numerous bite force models have been used to study the feeding behaviors of extant and extinct carnivores (e.g., Campbell and Santana, 2017; Christiansen and Wroe, 2007; Szalay, 1969; Therrien, 2005), clarifying the form and function of cranial and dental modifications, while also giving insights into their paleoecology (Emerson and Radinsky, 1980; Figueirido et al., 2013; Palmqvist et al., 2011; Slater and Van Valkenburgh, 2009; Tseng and Flynn, 2015). However, the skulls of herbivores are not frequently studied using bite force, or other biomechanical assessments (Button et al., 2014; DeSantis et al., 2020; Sharp, 2014). Most studies of bite force in herbivores are focused on rodents, broadly defined as a herbivorous group (Becerra et al., 2014; Freeman and Lemen, 2008; Maestri et al., 2016), albeit with highly derived masticatory morphology. To include a range of tapir species across a large temporal and phylogenetic scope, bite force calculations in this study were based on the 'dry skull' methodology (and associated assumptions) pioneered by Thomason (1991). A two-dimensional model was used to infer bite forces at each tooth in the upper toothrow. This method models muscle forces of the *m. masseter* + *m. pterygoideus* and *m. temporalis* as single force vectors acting vertically through the centroid, a uniform proxy for the measurement perpendicular to the plane of the cross-sectional area of the

muscles. The moment arm of each muscle (in-levers) is measured as the distance from the muscle centroid to the temporomandibular joint (Figure 2). By adding the moments of the jaw adductor muscles, dividing by the out-lever, and multiplying by two (to account for both sides of the mouth), the bilateral bite force at each location in the toothrow can be calculated.

Bilateral bite forces were estimated using the equation:

$$\text{Bite Force} = \frac{2 * (MP * mp + T * t)}{O_{\text{i}}}$$

where *MP* is the cross-sectional area for *m. masseter* + *m. pterygoideus*, *mp* is the moment arm for *m. masseter* + *m. pterygoideus*, *T* is the cross-sectional area for *m. temporalis*, *t* is the moment arm for *m. temporalis*, and O_{i} is the out-lever from the temporomandibular joint to each tooth.

Calculating bite forces for a clade with large body size differences between species can result in bite force profiles that only reflect size, rather than cranial biomechanics. Preliminary Reduced Major Axis (RMA) regressions, performed with the R package "lmodel2" (v.1.7.3) (Legendre, 2018), and Phylogenetic Generalized Least Squares (PGLS) regressions performed with the "caper" (v.1.0.1.) package (Orme et al., 2013) demonstrated that size bore a strong positive correlation with bite force at the species-level in tapirs (Figure S1a and S1d) (see also Results). While size is an informative aspect of feeding ecology, our intention here was to also investigate the bite force relative to specific aspects of skull shape (e.g., height of sagittal crest), and as such relative values were also calculated for that comparison. Thus, bite forces were corrected for size by dividing results by total skull length, a good proxy for body mass in mammals (Bertrand et al., 2016; Cassini et al., 2012; Reynolds, 2002) to provide relative bite forces. Mean maximal absolute and relative bite forces per species are listed in Table 2. Species averaged bite force profiles were produced for comparing species and used in phylogenetic analyses; individual species profiles demonstrating the range of bite force values for taxa including five or more specimens were also produced (Figure S2). Bite forces taken at the M1, near the center of the toothrow of full adult tapirs, are treated as maximal bite forces in this study to account for slight differences in ages between specimens.

The temporalis muscle and masseter-pterygoid muscle complex are the primary masticatory muscles, controlling the movement of the mandible. These masticatory muscles can act differently at different times in the chewing cycle. During mastication, the abducting *m. temporalis* and *m. masseter* work together to allow not only a vertical closing of the mouth but also to perform

controlled lateral movements of the jaw relative to the skull, because of their opposite effects on the transverse movements (Herring et al., 2001); the *m. temporalis* pulls backward and moves the mandible ipsilaterally, while the *m. masseter* pulls forward and moves the mandible contralaterally, making these muscles active in opposite side pairs ("diagonal couples") (Herring and Scapino, 1973; Herring et al., 2001). On the other hand, the *m. pterygoideus* will produce transverse (ectental) movement and it has a function in antagonizing the tendency of the masseter to evert the angle and lower border of the mandible during contraction (Hemae, 1967). During the chewing cycle, we see that first, the vertical movers are most important while later in the biting cycle the lateral movers will become more important for grinding the food. Different parts of the *m. temporalis* and *m. masseter* musculature are involved in these vertical and lateral movements. For example, the posterior part of the *m. temporalis*, the anterior part of the *m. masseter*, and the medial *m. pterygoid* generate the lateral jaw movements, while vertical movements are produced by the anterior *m. temporalis*, posterior *m. masseter* and zygomaticomandibularis (Gorniak, 1985). The different actions of the masticatory muscles warrant the bite forces to be tested separately as well as combined for overall bite force. Hence, bite forces were calculated for the *m. masseter* + *m. pterygoid* and *m. temporalis* separately and used in additional analyses (Figure S3). Muscle orientations and usage during mastication are based on generalised information available for ungulates, as no experimental information is available at this time for tapirs.

Tapirid Sagittal Crest

In this study, the sagittal crest height was measured from the posterior zygomatic arch to the tallest point on the skull (with toothrow horizontal) (Figure 2; this measurement acts as a proxy for fascicle length of temporalis muscle). Preliminary regressions (RMA and PGLS) of sagittal crest height vs. size (skull length) suggested a limited, but evident, influence of body size on crest height (Figure S1b and S1e). Sagittal crest height was therefore also corrected for size effects by dividing by total skull length, providing a relative sagittal crest value for comparisons with relative bite force and phylogeny. Table S2 demonstrates the mean absolute and relative sagittal crest height values per species.

All raw measurements and (relative) bite force calculations per specimen can be found in the Supplementary Information.

Phylogenetic Reconstruction

The phylogenetic relationships across all of Tapiridae are currently unresolved; however, the species examined in this study have been the subject of phylogenetic revision over the past 10 years, and relationships are for the most part well established (Cozzuol et al., 2013; Hulbert, 2010; Ruiz-García et al., 2016a; Ruiz-García et al., 2016b). A composite phylogenetic tree was compiled in Mesquite 3.6 (Maddison and Maddison, 2019) based on published tapirid topologies (Colbert, 2005; Cozzuol et al., 2013; Holanda and Ferrero, 2013; Hulbert, 2010; Hulbert and Wallace, 2005). The resultant informal topology retained monophyly of the *Helicotapirus* subgenus (Hulbert, 2010), with Asian *Tapirus* species as sister group to all New World tapirs (Figure S8). The informal tree was time-scaled using the "paleotree" package (Bapst, 2012) in R, based on first-last occurrence dates from the Palaeobiology Database (Behrensmeyer and Turner, 2013). The informal phylogeny can be found in the Supplementary Information.

Statistical Testing

All statistical analyses were performed in R v.3.6.1 (R Core Team, 2013), with significance at 95% (alpha $\leq$ 0.05). Bite force and sagittal crest analyses were performed with both the log-transformed raw values (to account for large differences in tapir size; see (MacLaren et al., 2018) and relative values. *Tapirus haysii* was excluded from the bite force vs. sagittal crest height regressions due to the specimen (ICVM 835/3365) exhibiting a very crushed sagittal crest. For the other analyses, the sagittal crest height of another specimen of *T. haysii* (UF 80446) was used; no lateral image was available for this specimen. Relative sagittal crest height was calculated by using the approximate skull length of specimen UF 80446 (representing only the neurocranium) based on the scaled *T. haysii* (ICVM 835/3365).

Differences in bite force and sagittal crest height between species were tested for using One-way Analysis Of Variance (ANOVA) with post-hoc Tukey's Pairwise comparisons. In cases of deviations from normality (tested for using Shapiro-Wilk Normality Test), the Kruskal–Wallis test by ranks was used with Pairwise Wilcoxon Rank Sum tests, with correction for multiple testing. ANOVAs, Shapiro-Wilk, Kruskal-Wallis and Wilcoxon Rank Sum tests were performed using the R package "stats" (v.3.6.1.). Significant differences in bite force and sagittal crest height between the Nearctic and Neotropical Pleistocene tapirs (Table 1) were tested for using a one-way ANOVA and a phylogenetic ANOVA (to establish the influence of phylogenetic relatedness on any observed differences) from the "geiger" (v.2.0.6.4) package in R (Harmon et al., 2008). Species means were used for these analyses rather than specimen measurements, as the latter would result in a skewed sample in favor of Neotropical specimens due to uneven sampling (Table 1).

Bite force (at M1) and sagittal crest height were tested for a phylogenetic signal using the "phytools" (v.0.6-99) package in R (Revell, 2012). Pagel's lambda (λ) was used as a test statistic, assessing a significant departure from λ = 0; lambda values close to 1 indicate high phylogenetic signal in the test variable, whereas values close to 0 suggest little or no influence of phylogenetic relatedness on the test variable (Pagel, 1999). Maximum likelihood ancestral states of bite force and sagittal crest height were estimated for all nodes and branches to illustrate the variation across the tree topology with the R package "phytools" (v.0.6.) (Revell, 2012). Finally, to infer whether estimated bite forces are lower in species with higher sagittal crests, phylogenetic generalized least squares (PGLS) regressions of maximum bite forces against sagittal crest height were performed.

Results

Cranial Bite Forces

Absolute (log-transformed) bite forces

Bite force profiles demonstrate the mean bite forces along the toothrow for every species (Figure 3). As expected, bite forces increase anteroposteriorly along the toothrow. *Tapirus augustus* shows the highest bite forces along the cranium overall, with *N. marslandensis* showing the lowest (closely followed by *P. simplex*). Within the extant tapir species, *T. indicus* exhibits the highest bite force (Figure 3a,b). Neotropical tapir species closely resemble each other in absolute bite forces, with *T. mesopotamicus* exhibiting the highest (Figure 3d). Within Nearctic tapirs, the highest bite forces are found in *T. veroensis* (Figure 3c). Bite force ranges for species with multiple specimens suggest that *T. terrestris* (n=30) exhibits the greatest range of bite forces, whereas *T. kabomani* (n = 7) displays more conservative bite force ranges (with one outlier) (Table 1; Figure S2). The large sample of *T. terrestris* specimens suggests this result may be affected by sample size. Regressions of bite force with skull length (proxy for body size) indicate a significant positive relationship ($p < 0.05$) and high predictive power for skull length determining tapirid bite force (RMA: $R^2 = 0.81$ and PGLS: $R^2 = 0.77$) (Figure S1a and Figure S1d).

When bite force profiles of the *m. temporalis* and *m. masseter* + *m. pterygoideus* were assessed separately (Figure S3), results suggest that both *T. augustus* and *T. mesopotamicus* have a higher relative contribution to overall bite force from the *m. masseter* + *m. pterygoideus* than other species; excluding these two species, all other tapirids in the study exhibit notably higher contributions to overall bite forces from the *m. temporalis*. Similar to the total bite force, a size

effect is present (Figure S4a) (RMA: $p < 0.05$); size is more strongly correlated with the *m. masseter* + *m. pterygoideus* (RMA: $R^2 = 0.76$) than the *m. temporalis* (RMA: $R^2 = 0.69$) muscle forces.

The absolute bite forces of the specimens were not normally distributed ($W = 0.96$, $p < 0.05$), so the non-parametric Kruskal-Wallis test was employed. The Kruskal-Wallis test results indicate significant differences in cranial bite forces across all tooth bite points for the entire sample (all $p < 0.05$). Pairwise Wilcoxon Rank Sum tests between species indicate a significant difference in bite force across all tooth bite points between *T. indicus* vs. *T. terrestris* (all $p < 0.05$), *T. pinchaque* (all $p < 0.05$), and *T. kabomani* (all $p < 0.05$); these are the comparisons with the highest sample sizes (Table 2). Wilcoxon Rank Sum and Signed Rank Tests and phylogenetic ANOVAs both showed no clear differences in bite forces between Pleistocene tapir species from the Nearctic and the Neotropical (all $p > 0.05$).

Relative bite forces

When compared to the absolute bite forces, similar patterns in bite force profiles are found for the relative bite forces of the species (Table 2). *T. mesopotamicus* shows the highest relative bite forces in the cranium overall, (Table 2). Within the extant species, *T. indicus* again exhibits the highest relative bite forces, which when calculated relative to skull length are nearly equal to the relative bite forces of the much larger *T. augustus* (Table 2). Similar to the absolute bite forces, *T. mesopotamicus* has the highest relative bite force within Neotropical tapirs. In Nearctic tapirs, *T. johnsoni* has the highest relative bite forces, while *N. marslandensis* and *P. simplex* again show the lowest.

The relative bite forces of the specimens were not normally distributed ($W = 0.92$, $p < 0.05$). The Kruskal-Wallis test indicates species differences in relative cranial bite forces across all bite points (all $p < 0.05$). Pairwise Wilcoxon Rank Sum tests between species indicate a significant difference in relative bite force across all tooth bite points between *T. terrestris* and *T. indicus* (all $p < 0.05$); this is the only interspecific comparison with sufficient sample size to provide a significant statistical comparison (Table 2). Wilcoxon Rank Sum and Signed Rank Tests and phylogenetic ANOVA both showed no clear differences in relative bite forces between Pleistocene tapir species from the Nearctic and the Neotropics (all $p > 0.05$).

Sagittal Crest

Absolute sagittal crest height

Tapirus augustus has the highest sagittal crest (measured from the caudal-most point of the zygomatic arch), and *N. marslandensis has* the lowest (Table S2). Mean sagittal crest height for individual species with more than six specimens suggest that *T. pinchaque* exhibits the largest range of sagittal crest height values, whereas *T. indicus* displays the most restricted range of values (Table S2). Regressions of sagittal crest height against skull length (a proxy for size) indicated a strong positive relationship ($p < 0.05$), but a low to moderate predictive power of skull length for determining sagittal crest height (RMA: $R^2 = 0.58$ and PGLS: $R^2 = 0.66$) (Figure S1b and Figure S1e).

Sagittal crest heights of the specimens are not normally distributed ($W = 0.91$, $p < 0.05$). Kruskal-Wallis testing indicated overall differences in sagittal crest height ($p < 0.05$). Results of Tukey's Pairwise comparisons (Table S3) suggest the most closely related living tapirs, *T. terrestris* and *T. pinchaque* (Cozzuol et al., 2013; Ruiz-García et al., 2012), differ significantly in sagittal crest height ($p < 0.05$). In addition, also *T. terrestris* and *T. indicus* differ significantly in sagittal crest height ($p < 0.05$) (Table S3). One-way ANOVA and phylogenetic ANOVA indicated no clear difference in sagittal crest height between Nearctic and Neotropical Pleistocene tapir species ($p > 0.05$); however, the removal of the low-crested *T. pinchaque* from the Neotropical group yielded a value for ANOVA trending toward significance ($p = 0.056$), although this signal was reduced when tested using phylANOVA ($p = 0.28$).

Relative sagittal crest height

Tapirus mesopotamicus exhibits the highest mean relative sagittal crest height, and *N. marslandensis* the lowest (Table S2). Mean relative sagittal crest height for individual species with more than six specimens suggest that *T. kabomani* exhibits the largest range of relative sagittal crest height values, whereas *T. indicus* and *T. terrestris* display the most restricted range of values (Table S2). Relative sagittal crest height is normally distributed ($W = 0.99$, $p > 0.05$). ANOVA suggests overall significant differences in relative sagittal crest height were found across the whole sample ($F_{(10,13)}=10.15$, $p < 0.01$). Results of Tukey's Pairwise comparisons (Table S4) suggest also that *T. terrestris* and *T. pinchaque* differ significantly in relative sagittal crest height ($p < 0.05$), as they did for absolute crest height. All results of Tukey's Pairwise comparisons are found in Table S4. One-way ANOVA and phylogenetic ANOVA results for differences in relative sagittal crest height between Nearctic and Neotropical Pleistocene tapir species are displayed in Table 3. When including all Pleistocene tapirs from these two biogeographical realms, no differences are found in sagittal crest height ($p > 0.05$). However, after the exclusion of the low-crested *T. pinchaque* from the Neotropical group, we show that Neotropical tapirs have

significantly higher sagittal crests than Nearctic species ($p < 0.05$). This result is no longer supported after accounting for phylogenetic relatedness in the phylANOVA ($p > 0.05$) (Table 3).

Phylogenetic Comparisons and Relationship between Sagittal Crest Height and Bite Force

Maximal absolute bite forces (at M1) are plotted on the informal phylogeny in Figure 5a, demonstrating that non-*Tapirus* species (*Protapirus*, *Nexuotapirus*) have low bite forces compared to *Tapirus*-species. Sister taxa in general exhibited similar absolute bite forces (e.g., *T. terrestris* and *T. pinchaque; T. augustus* and *T. indicus;* and *T. veroensis* and *T. haysii*). Relative bite forces at M1 are plotted on the informal phylogeny in Figure 5b, allowing a visual comparison between absolute and relative bite force across the tapirid phylogeny. The patterns closely resemble one another; however, the comparison between the absolute and relative bite forces clearly demonstrates differences for *T. mesopotamicus*, which exhibits a very high relative bite force but comparably mid-ranged absolute bite force. The Indo-Malayan *T. indicus* and *T. augustus* exhibit the highest absolute bite forces, but not the highest bite forces relative to their size. Both absolute bite force and relative bite force exhibit a strong phylogenetic signal ($\lambda = 0.96$, $p < 0.05$; $\lambda = 0.99$, $p < 0.05$).

Relative sagittal crest heights are plotted onto the informal phylogeny in Figure 5c. With the notable exception of *T. pinchaque*, most Neotropical tapirs (*T. bairdii, T. terrestris, T. kabomani, T. mesopotamicus,* and *T. rondoniensis*) show the highest relative sagittal crests in the sample by comparison to the Indo-Malayan and Nearctic species. Relative sagittal crest height does not exhibit a significant phylogenetic signal ($\lambda = 0.35$, $p > 0.05$); however, after excluding *T. pinchaque*, relative sagittal crest height exhibits a significant phylogenetic signal ($\lambda = 0.69$, $p < 0.05$). The non-corrected, absolute sagittal crest height exhibits a significant phylogenetic signal, both with *T. pinchaque* included ($\lambda = 0.84$, $p < 0.05$) and excluded ($\lambda = 0.95$, $p < 0.05$) .

The PGLS regression between log-transformed absolute bite forces (at M1) and absolute sagittal crest heights per species found a significant relationship between the traits while accounting for phylogenetic relatedness ($F_{(1,12)} = 50.81$, $R^2 = 0.79$, $p < 0.05$) (Figure 6a). The same relationship was found when an RMA regression was performed ($R^2 = 0.67$, $p < 0.05$), suggesting that phylogeny was not a factor in the relationship between non-size corrected bite force and sagittal crest height (Figure S1c and Figure S1f). RMA regressions of *m. temporalis* and *m. masseter* + *m. pterygoideus* against sagittal crest height of the species indicated a positive relationship between sagittal crest height and bite force for both sets of muscles (all $p < 0.05$) (Figure S4b).

However, sagittal crest height is a poor predictor for *m. temporalis* bite force ($R^2 = 0.54$), whereas for *m. masseter* + *m. pterygoideus*, the predictive power is higher ($R^2 = 0.74$).

The PGLS regression between species-averaged relative bite forces (at M1) and relative sagittal crest heights found no significant relationship between the size-corrected traits ($F_{(1,12)} = 0.72$, $p = 0.41$) (Figure 6b).

Discussion

In this study, we investigated bite forces and sagittal crest heights across a broad range of tapirs to determine in a quantitative manner whether sagittal crest height is correlated with bite forces across a large phylogenetic scope. In addition, patterns of variation in bite forces and sagittal crest heights among tapir species exploiting different biogeographical realms were also investigated.

The Relationship Between Bite Force and Sagittal Crest Height

Our study showed that tapirs exhibit variation in bite forces, with some species having higher bite forces relative to their skull size than might be expected (e.g., *T. mesopotamicus*). Unsurprisingly, tapirs with large skulls (and consequently large muscle masses) had high absolute bite forces. Bite force estimates for large herbivores are rare, particularly for extant ungulates (e.g., DeSantis et al. 2020; bite forces calculated but not reported), hence it is quite difficult to see how these tapir bite forces compare to other extant clades of large herbivores. However, bite force estimates have been calculated for large, extinct herbivores such as the diprotodontid marsupial *Diprotodon optatum* (Sharp and Rich, 2016) and the hystricognath rodent *Josephoartigasia monesi* (Blanco et al., 2012). When compared to mid-sized tapirids in the present study (e.g., *T. bairdii*, *T. veroensis*; body masses ± 250kg, MacLaren et al. 2018), the estimation of bilateral bite force at the centre of the cheek toothrow for *D. optatum* yields similar bite forces (5000-6000 N) despite *D. optatum* reputedly reaching body masses of over 2000 kg (Wroe et al., 2004). Bilateral bite forces at the caniniform incisor for mid-sized tapirs (2000-2700 N) fall well within the range of bite forces for the giant rodent *J. monesi* (1260-6428 N; values from Blanco et al. 2012 scaled up to assume a bilateral bite force). Although these values for herbivores may appear high, especially for tapirs, herbivorous species of bears (*Ursus malayanus* and *Ailuropoda melanoleuca*) exhibit higher bite forces than carnivorous species (Christiansen and Wroe, 2007); the overall pressure exerted on the apex of sharp, carnivoran teeth will ultimately be greater for a given input force than that of a ridged or lophodont tooth, as are exhibited in tapirs. Thus, the high values calculated for large-bodied herbivores, in general, may not be overly surprising. However, it must be stressed that although tapirs, rodents and marsupials are all hind-gut fermenters (Sanson, 2006),

comparisons between masticatory biomechanics made here do not account for variation in muscular arrangement and architectures between these clades, and should be interpreted with a great deal of caution. Systematic investigations into modern herbivorous ungulate species and communities, like those of the African savanna or American woodlands, will likely yield far more valid inter-clade comparative data.

For tapirs with large skulls (e.g., *T. augustus* and *T. mesopotamicus*), the combined *m. masseter* + *m. pterygoideus* bite force estimates contribute more to their very high bite forces than is exhibited by other species. The majority of tapirs in this study have a more dominant contribution from the *m. temporalis*, which originates from the sagittal crest. Recent biomechanical analyses proposed that tapirs with high sagittal crests are not specialized for high bite forces and hard-food processing (DeSantis et al., 2020). Our results partially support the conclusions of DeSantis et al. (2020), which was restricted to only five specimens of *Tapirus*. High sagittal crests are not correlated with high cranial bite force in the Tapiridae after taking into account body size. Absolute sagittal crest height also represents a relatively poor predictor for bite force in tapirs (when phylogeny is not taken into account), with 33% of tapir species exhibiting different (higher or lower) bite forces than predicted from their sagittal crest height alone (Figure S1c). When phylogenetic relatedness is taken into account, the predictive power increases, with only 21% of tapir species poorly predicted (Figure 6a). However, when accounting for size and species relatedness, no correlation exists between relative bite force and relative sagittal crest height (Figure 6b). This apparent decoupling of bite force and sagittal crest height relative to size in tapirids is in stark contrast with the pattern generally found in mammals with notable sagittal crests and hard foods in their diets (e.g., carnivores, rodents, primates) (Becerra et al., 2014; Randau et al., 2013; Tanner et al., 2008; Van Valkenburgh, 2007; Vogel et al., 2014). In many of these species, an expansion of the attachment area for the *m. temporalis* muscles allow for greater force application for processing hard objects (Van Valkenburgh, 2007). Our study demonstrates that osteological morphologies associated with particular behavior in certain groups, e.g., carnivorans, should not be translated to other species, such as tapirs, without validation, especially across trophic levels (i.e., from carnivores to herbivores). Many-to-one mapping of phenotype to function can lead to different trait combinations generating the same functional output (Thompson et al., 2017; Wainwright et al., 2005); equally, similar trait combinations may not achieve the same function in different phenotypes, e.g., osteological features such as high sagittal crests do not signify high bite forces in tapirs in the same way that they are known to do for carnivorans. It is likely that specific aspects of the carnivoran temporal musculature (e.g., physiological cross-sectional area) differ from those of tapirs, and potentially to ungulates in general. In addition, bite force alone can be an inadequate indicator of chewing performance, and other aspects need to be

taken into account to completely understand the relationship between sagittal crest height and bite force. For example, chewing performance can be influenced by factors such as muscle fiber type composition (Holmes and Taylor, 2021), morphology of dental occlusal surface (Koc et al., 2010), tooth material properties (Herbst et al., 2021), and jaw kinematics during mastication (Kuninori et al., 2014). It is important to take into account that the dry-skull method used in this study has its limitations (Bates et al., 2021; Ellis et al., 2008; Law and Mehta, 2019), including over- or underestimation of muscle physiological cross-sectional area and underestimation of bite force. For comparative purposes, in this study, the method models muscle forces as vertically oriented single force vectors. This is a simplification of reality; muscle actions are invariably not vertical, they are determined by the location and size of the attachment site, and anatomy and composition of the muscles. The vector orientations can lead to an over- or underestimation of bite force (Cox et al., 2015), and these error rates can vary between taxa (Bates et al., 2021). Unfortunately, an evaluation of the accuracy of muscle-area assessment techniques and vector orientations is currently lacking for tapirs. It should also be noted that fiber lengths and pennation angles were not calculated in this study; as both these architectural properties are known to influence force-generating capacity in muscles (Lieber and Fridén, 2000), it is possible that our estimates for *m. temporalis, m. masseter* and *m. pterygoideus* bite forces do not reflect reality. However, the uniformity of the image orientation utilized in this study, and the comparative nature of the investigation in general, offers a solid basis for comparisons within the clade, if not necessarily beyond the Tapiridae.

The (relative) height of the sagittal crest being poorly correlated with (relative) cranial bite force within the Tapiridae (Figure 6) suggests an alternative function for pronounced sagittal crests in this group. As hypothesized by DeSantis et al. (2020), the presence of large sagittal crests may be indicative of temporalis muscles with long fibers conferring benefits for prolonged processing of tough fodder. Recently, the stiffness and toughness of the diet were found to be related to both chewing investment and chewing duration in llamas (Nett et al., 2021); this may thus also apply to tapirs. A pronounced sagittal crest in tapir skulls leads to higher stress loads when feeding on hard objects (DeSantis et al., 2020); thus, needing to confer high bite forces would not be beneficial. Hence, diet may have shaped sagittal crest height in tapirids, with tough, folivorous diets requiring large sagittal crests and associated temporalis musculature with long fibers for prolonged mastication, rather than high bite forces for, for example, crushing hard-shelled seeds; similar to the findings in llamas (Nett et al., 2021). In tapirs with a sagittal table or low sagittal crests, such as *T. indicus* (Dumbá et al., 2018), hard plant material such as thick-walled seeds are more prevalent in the diet (Campos-Arceiz et al., 2012). Dietary information on extant species from ecological studies (Downer, 2001; Henry et al., 2000; Janzen, 1982; O'Farrill et al., 2013),

and finite element analysis and dental microwear texture analysis (DeSantis et al., 2020) confirm these assumptions, and our results tally with these previous studies albeit from a different experimental angle.

Tapir Size as a Factor

Bite force is strongly correlated with skull size in our analysis, suggesting that tapir size is indicative of its potential bite force and potential diet (e.g., hard vs. soft plant material). The methodology used in this study to calculate bite force is inherently linked to size, as bite force is influenced by the distance from the muscle vector and jaw joint (TMJ), and the distance from the tooth to the jaw joint (Nabavizadeh, 2016; Thomason, 1991); these distances differ between tapirs of different sizes. The body size – bite force relationship appears to be uniform within the *Tapirus* genus; the conservation of bite force within *Tapirus* would therefore have offered a stable performance foundation within their relatively conservative niche (forest megaherbivore) throughout much of their evolutionary history. This inherent stability would have then facilitated their expansion into different, drier habitats during the Pliocene/Pleistocene (cf. mesoeucrocodylians, Gignac et al., 2021).

Sagittal crest height also correlates with tapir size; however, this relationship is less strong than the one between size and bite force (Figure S1a,d vs. S1b,e). Neotropical tapirs (with the exception of *T. pinchaque*), display high sagittal crests for their size, with a positive allometric relationship revealed for this group of Pleistocene taxa (Figure S1). The high-crested Neotropical species are notably separate from the other tapir taxa, and in relative terms, these species have much higher sagittal crests than other species within the family (Figure 5; see also Dumbá et al., 2018). As a result, when all tapirs are considered, a general predictive relationship that tapir size is indicative of its sagittal crest height cannot be maintained. However, this pattern is particularly driven by the presence of positive allometry in sagittal crest height for Pleistocene tapirs in the Neotropical biological realm.

New World tapir cranial morphology and performance during the Pleistocene

Tapirs present in the Neotropical realm, including Central and South America, during the Pleistocene exhibit large variability in bite force (Figure 3 and 4). The range of skull morphologies in this group (including *T. bairdii, T. kabomani, T. terrestris, T. rondoniensis, T. mesopotamicus,* and *T. pinchaque*; Figures 3 and 5) are also quite disparate, even among just three of the extant species (*T. pinchaque*, *T. bairdii,* and *T. terrestris*; Figures 3 and 5). This variation in skull shape and performance may represent a mechanism to avoid excess interspecific competition or niche

overlap (Button et al., 2014; Franco-Moreno et al., 2020; Gordon and Illius, 1989; Klein and Bay, 1994; Leuthold, 1978; Shipley et al., 1994). For extant tapirs in the Neotropics, this is not an issue that may drive divergence in biting capacity, as their ranges rarely overlap (Figure 4; see also Lizcano et al., 2002); however, cohabitation by contemporaneous Neotropical species in the Pleistocene may yet have driven the differences in bite force we observe in our results. For example, the now extinct *T. mesopotamicus* overlaps in geographical range with *T. terrestris*, with both taxa seemingly present in the latest Pleistocene (Cozzuol et al., 2013; Ferrero and Noriega, 2007) (Figure 4). *Tapirus mesopotamicus* has a high predicted maximal bite force, especially compared to the similarly-sized *T. rondoniensis*, *T. pinchaque,* and *T. terrestris* (Figure 4; Figure S1a). Compared to the other Pleistocene South American species, this high bite force may have enabled *T. mesopotamicus* to specialize on (or at least consume) harder food items such as large, thick-walled seeds. At the very least, *T. mesopotamicus* appears to have been capable of feeding on items which modern Neotropical tapirs with comparable skull sizes would be unable to (Figure S1); this would potentially have allowed *T. mesopotamicus* and contemporaneous tapirs to partition resources and avoid competition. Similarly, *T. kabomani* has the lowest bite forces within the Neotropical realm; tapir species overlapping in geographic range, such as *T. terrestris* and *T. rondoniensis* (Figure 4), exhibit higher bite forces; again, this potentially facilitates niche differentiation, with the smaller *T. kabomani* likely feeding on softer fruit, leaves and green shoots whereas the larger species would be able to break apart small seeds and chew for prolonged periods on woody twigs (DeSantis et al., 2020). Nearctic tapirs also seem to exhibit these patterns, as *T. lundeliusi* has a lower bite force compared to other similar-sized species such as *T. pinchaque* (MacLaren et al., 2018) than the species which it overlaps in geographic range, i.e., *T. veroensis* and *T. haysii* (Figure 4). Similar conclusions have also been drawn for sauropods in the Late Jurassic Morrison Formation (Button et al., 2014), ornithischian dinosaurs (Nabavizadeh, 2016), sea otters (Campbell and Santana, 2017), and sea lions and seals (Franco-Moreno et al., 2020). It is thus possible that the biomechanical differences between tapirids revealed in this study contributed to niche differentiation to avoid interspecific competition, although more detailed studies on the comparative structural composition of the vegetative intake of modern tapirs would be required to support this.

Several species with the highest bite forces appear in Eurasia, North America, and South America around the onset of the Pleistocene epoch (*T. mesopotamicus,* Ferrero and Noriega, 2007; *T. augustus* Matthew and Granger, 1923; and *T. veroensis* Sellards, 1918), when the planet was descending into a glacial period (Pisias and Moore, 1981; Van der Hammen, 1974). In absolute terms, Pleistocene *Tapirus* have far higher bite forces compared to geologically earlier species (e.g., *T. polkensis* and *T. johnsoni*: Figure 5a); this pattern holds when skull size is taken into

account (Figure 5b), and we interpret these higher bite forces in Pleistocene tapirs as independent of the gradual increase in overall body size observed in tapirs through time (Franzen, 2010; Radinsky, 1965). Wetter and drier climates alternated throughout the Pleistocene, causing fluctuations in vegetation cover and composition (Van der Hammen, 1974). A drier climate with less moisture in the soil available for plants may have resulted in a cascade effect in primary consumers, influencing the evolution of bite forces in Pleistocene tapirs for them to take advantage of nutritious seeds and more fibrous vegetation, in addition to traditionally softer foliage associated with brachydont browsers. Further investigation into the plant material available to different species may shed more light on this potential selection pressure for higher bite forces in Pleistocene tapirs.

Our results for Pleistocene tapirs also suggest that there is a morphological signal in sagittal crest height between the Neotropical and Nearctic tapirs (Figure 4). This signal is strongly influenced by phyletic heritage and is tempered by the presence of the low-crested *T. pinchaque* in the montane páramo forest of the Neotropical realm (Padilla et al., 2010). Both relative and absolute sagittal crest values suggest strong (if not significant; Table 3) differences between the morphologies of tapir sagittal crest height in the two realms. However, the fact that the two groups represent separate lineages along our informal tapir phylogeny (Figure 5), and the strength of the signal is heavily affected by the exclusion/inclusion of *T. pinchaque* (Table 3), suggests that there is insufficient ecological or phylogenetic resolution to state anything concrete about the effect of phylogeny or realm occupation on sagittal crest morphology in tapirs. Taking phylogenetic relationships into account when looking at morphology and performance is essential, as this can lead to divergent results if they are (not) accounted for, as we have demonstrated in our results. Accurate, comprehensive phylogenies incorporating many powerful characters from both molecular and morphological outlooks are required, something that is currently lacking for tapirs.

Nonetheless, the morphology of *T. pinchaque* clearly departs from other Neotropical species with regard to their skull shape and sagittal crest height. The species closely resembles Pleistocene Nearctic tapirs with a low, narrow sagittal crest (see also Dumbá et al., 2018). *Tapirus pinchaque* not only differs in skull shape compared to other extant tapir species but also exhibits morphological divergence in their postcranial skeleton as well (MacLaren and Nauwelaerts, 2016; MacLaren and Nauwelaerts, 2017; MacLaren et al., 2018). The divergent morphology of *T. pinchaque* may be linked to their unique ecology. As the name implies, *T. pinchaque,* or the mountain tapir, occurs at higher elevations (between 1.100 – 1.400 m); it is a characteristic species from the Andean temperate rainforest and páramo wetlands which are characterized by cold and humid zones with thick bushes (Acosta et al., 1996; Downer, 1996; Padilla et al., 2010). The bite

force of *T. pinchaque* is comparable to the other Neotropical extant species (Figure 3), suggesting force application is not a selection pressure for a lower sagittal crest. Moreover, molecular and morphological phylogenetic studies (Cozzuol et al., 2013; Ruiz-García et al., 2012; Ruiz-García et al., 2016b) suggest that the split between *T. pinchaque* and *T. terrestris* occurred very recently, after the onset of the Pleistocene glaciation, implying a common, high-crested ancestor for both taxa. It is possible that selection pressures of the unique habitat of *T. pinchaque*, such as lower temperatures and/or higher elevations may have driven the evolution of the lower sagittal crest in *T. pinchaque* by comparison to its closest relatives. The exact influences of temperature on cranial morphology of large mammalian herbivores are unknown, and further research into this may provide more empirical evidence supporting this claim, which at present remains only a speculative theory.

In conclusion, our results demonstrate that, within the Tapiridae, sagittal crest height is poorly correlated with cranial bite force (when corrected for body size), suggesting an alternative driver and function for pronounced sagittal crests in comparison to carnivorans (e.g., prolonged mastication). Tapirs exhibit variation in bite force and sagittal crest height across their phylogeny and different biogeographical realms. The high-crest morphology appears repeatedly in the tapir fossil record, focused mostly in the Neotropical species. The highest absolute bite forces within tapirs appear to be driven by estimates for the masseter – pterygoid muscle complex, rather than predicted forces for the temporalis muscle. Further research into the muscular architecture of the masticatory apparatus in tapirs (and other megaherbivores) may offer more detailed explanations for the differences we observe. Bite forces in tapirs seem to peak in the Pleistocene, independent of body size, suggesting potential dietary shifts as a result of climatic changes (ecosystem drying) during this epoch. In particular, the divergent biomechanical capabilities of different contemporaneous tapirids may have contributed to niche differentiation, allowing multiple species to occupy overlapping territories. The apparent morphological and performance-based adaptability of this group to warmer and cooler temperatures, facilitated to some extent by a stable bite performance during feeding, have enabled tapirs to remain key components of many tropical and temperate ecosystems throughout the Neogene.

Acknowledgements

The authors wish to thank C. Cartelle (Museu de Ciências Naturais PUC Minas), L. F. B. Flamarion (Coleção de Mastozoologia do Museu Nacional do Rio de Janeiro), F. A. Perini (Coleção de Mastozoologia da Universidade Federal de Minas Gerais), O. Pauwels (Royal Belgian Institute of Natural Sciences), J. Lésur (Museum National d'Histoire Naturelle), L.

Tyteca (MuseOs Natuurhistorichmuseum) and R. C. Hulbert Jr. (Florida Museum of Natural History) for the access to tapir collections. This study was conceived by JAM. Measurements were collected by LVL, KS and JAM; first-hand images were provided by LCCSD, MAC and JAM. Statistical analyses were performed by LVL; drafts were written by LVL and KS, with all authors contributing to the final version of the manuscript. This work was facilitated by doctoral and post-doctoral funding awarded to JAM (doctoral by the Fonds Wetenschappelijk Onzerzoek [FWO]; post-doctoral by Fonds de la Recherche Scientifique [FNRS]; travel grant from the Florida Museum of Natural History [FLMNH]), and a doctoral fellowship awarded to LCCSD (by the Coordenação de Aperfeiçoamento de Pessoal de Nível Superior [CAPES]).

The authors have no conflicts of interest to declare.

References

Acosta, H., Cavelier, J. and Londono, S. (1996). Aportes al Conocimiento de la Biologia de la Danta de Montana, Tapirus pinchaque, en los Andes Centrales de Colombia. *Biotropica* **28**, 258–266.

Bapst, D. W. (2012). Paleotree: An R package for paleontological and phylogenetic analyses of evolution. *Methods Ecol. Evol.* **3**, 803–807.

Bates, K. T., Wang, L., Dempsey, M., Broyde, S., Fagan, M. J. and Cox, P. G. (2021). Back to the bones: Do muscle area assessment techniques predict functional evolution across a macroevolutionary radiation? *J. R. Soc. Interface* **18**, 1–8.

Becerra, F., Echeverría, A. I., Casinos, A. and Vassallo, A. I. (2014). Another one bites the dust: Bite force and ecology in three caviomorph rodents (Rodentia, Hystricognathi). *J. Exp. Zool. Part A Ecol. Genet. Physiol.* **321**, 220–232.

Behrensmeyer, A. K. and Turner, A. (2013). Taxonomic occurrences of Tapiridae recorded in the Paleobiology Database. Fossilworks. http://fossilworks.org.

Bertrand, O. C., Schillaci, M. A. and Silcox, M. T. (2016). Cranial dimensions as estimators of body mass and locomotor habits in extant and fossil rodents. *J. Vertebr. Paleontol.* **36**, e1014905.

Blanco, R. E., Rinderknecht, A. and Lecuona, G. (2012). The bite force of the largest fossil rodent (Hystricognathi, Caviomorpha, Dinomyidae). *Lethaia* **45**, 157–163.

Brünnich, M. T. (1772). Zoologiæ fundamenta prælectionibus academicis accomodata.

Button, D. J., Rayfield, E. J. and Barrett, P. M. (2014). Cranial biomechanics underpins high sauropod diversity in resource-poor environments. *Proc. R. Soc. B Biol. Sci.* **281**, 1–9.

Campbell, K. M. and Santana, S. E. (2017). Do differences in skull morphology and bite performance explain dietary specialization in sea otters? *J. Mammal.* **98**, 1408–1416.

Campos-Arceiz, A., Traeholt, C., Jaffar, R., Santamaria, L. and Corlett, R. T. (2012). Asian Tapirs Are No Elephants When It Comes To Seed Dispersal. *Biotropica* **44**, 220–227.

Cassini, G. H., Vizcaíno, S. F. and Bargo, M. S. (2012). Body mass estimation in Early Miocene native South American ungulates: A predictive equation based on 3D landmarks. *J. Zool.* **287**, 53–64.

Christiansen, P. and Wroe, S. (2007). Bite forces and evolutionary adaptations to feeding ecology in carnivores. *Ecology* **88**, 347–358.

Colbert, M. W. (2005). The facial skeleton of the early Oligocene Colodon (Perissodactyla, Tapiroidea). *Palaeontol. Electron.* **8**, 1–27.

Colbert, M. W. (2006). *Hesperaletes* (Mammalia: Perissodactyla), a new tapiroid from the middle Eocene of southern California. *J. Vertebr. Paleontol.* **26**, 697–711.

Cox, P. G., Rinderknecht, A. and Blanco, R. E. (2015). Predicting bite force and cranial biomechanics in the largest fossil rodent using finite element analysis. *J. Anat.* **226**, 215–223.

Cozzuol, M. A., Clozato, C. L., Holanda, E. C., Rodrigues, F. H. G. G., Nienow, S., de Thoisy, B., Redondo, R. A. F. F. and Santos, F. R. (2013). A new species of tapir from the Amazon. *J. Mammal.* **94**, 1331–1345.

Currey, J. D. (2006). *Bones: Structure and Mechanics*. Princeton University Press.

Czaplewski, N. J., Puckette, W. L. and Russell, C. (2002). A Pleistocene tapir and associated mammals from the southwestern Ozark Highland. *J. Cave Karst Stud.* **64**, 97–107.

Davis, J. L., Santana, S. E., Dumont, E. R. and Grosse, I. R. (2010). Predicting bite force in mammals : two-dimensional versus three-dimensional lever. *J. Exp. Biol.* **213**, 1844–1851.

de Soler, B. G., Vall-llosera, G. C., van der Made, J., Oms, O., Jordi, A. B., Sala, R., Blain, H.-A., Casas, F. B., Claude, J., Catalán, S. G., et al. (2012). A new key locality for the Pliocene vertebrate record of Europe: the Camp dels Ninots maar (NE Spain). *Geol. Acta* **10**, 1–17.

Demes, B. (1982). The resistance of primate skulls against mechanical stresses. *J. Hum. Evol.* **11**, 687–691.

DeSantis, L. R. G. (2011). Stable Isotope Ecology of Extant Tapirs from the Americas. *Biotropica* **43**, 746–754.

DeSantis, L. R. G., Sharp, A. C., Schubert, B. W., Colbert, M. W., Wallace, S. C. and Grine, F. E. (2020). Clarifying relationships between cranial form and function in tapirs, with implications for the dietary ecology of early hominins. *Sci. Rep.* **10**, 1–11.

Desmarest, A. G. (1819). Tapir l'inde, *Tapirus indicus*. *Nouv. Dict. d'histoire Nat. appliquée aux arts, à l'agriculture, à l'économie Rural. Domest. à la médecine. Paris Deterville.* 458.

Downer, C. C. (1996). The mountain tapir, endangered 'flagship' species of the high Andes. *Oryx* **30**, 45–58.

Downer, C. C. (2001). Observations on the diet and habitat of the mountain tapir (*Tapirus pinchaque*). *J. Zool.* **254**, 279–291.

Dumbá, L. C. C. S., Parisi Dutra, R. and Cozzuol, M. A. (2018). Cranial Geometric Morphometric Analysis of the Genus *Tapirus* (Mammalia, Perissodactyla). *J. Mamm. Evol.* **26**, 545–555.

Ellis, J. L., Thomason, J. J., Kebreab, E. and France, J. (2008). Calibration of estimated biting forces in domestic canids: Comparison of post-mortem and in vivo measurements. *J. Anat.* **212**, 769–780.

Emerson, S. B. and Radinsky, L. (1980). Functional Analysis of Sabertooth Cranial Morphology. *Paleobiology* **6**, 295–312.

Engels, S. and Schultz, J. A. (2019). Evolution of the power stroke in early Equoidea (Perissodactyla, Mammalia). *Palaeobiodiversity and Palaeoenvironments* **99**, 271–291.

Ferrero, B. S. and Noriega, J. I. (2007). A new upper Pleistocene tapir from Argentina: Remarks on the phylogenetics and diversification of neotropical Tapiridae. *J. Vertebr. Paleontol.* **27**, 504–511.

Figueirido, B., Tseng, Z. J. and Martín-Serra, A. (2013). Skull Shape Evolution In Durophagous Carnivorans. *Evolution (N. Y).* **67**, 1975–1993.

Franco-Moreno, R. A., Polly, P. D., Toro-Ibacache, V., Hernández-Carmona, G., Aguilar-Medrano, R., Marín-Enríquez, E. and Cruz-Escalona, V. H. (2020). Bite Force in Four

Pinniped Species from the West Coast of Baja California, Mexico, in Relation to Diet, Feeding Strategy, and Niche Differentiation. *J. Mamm. Evol.* 307–321.

Franzen, J. L. (2010). Pseudo Horses and Relatives of Horses. In *In. The Rise of Horses: 55 Million Years of Evolution.*, pp. 145–164. Johns Hopkins University Press, Baltimore.

Freeman, P. W. and Lemen, C. A. (2008). A simple morphological predictor of bite force in rodents. *J. Zool.* **275**, 418–422.

Gignac, P. M. and Erickson, G. M. (2016). Ontogenetic bite-force modeling of *Alligator mississippiensis*: implications for dietary transitions in a large-bodied vertebrate and the evolution of crocodylian feeding. *J. Zool.* **299**, 229–238.

Gignac, P. M., Smaers, J. B. and O'Brien, H. D. (2021). Unexpected bite-force conservatism as a stable performance foundation across mesoeucrocodylian historical diversity. *Anat. Rec.* 1–15.

Gill, T. N. (1865). October 10th. *Proc. Acad. Nat. Sci. Philadelphia (ed. Bridg. R.).* **17**, 183.

Gordon, I. J. and Illius, A. W. (1989). Resource partitioning by ungulates on the Isle of Rhum. *Oecologia* **79**, 383–389.

Gorniak, G. C. (1985). Trends in the actions of mammalian masticatory muscles. *Integr. Comp. Biol.* **25**, 331–338.

Graham, R. W., Grady, F. and Ryan, T. M. (2019). Juvenile Pleistocene tapir skull from Russells Reserve Cave, Bath County, Virginia: Implications for cold climate adaptations. *Quat. Int.* **530–531**, 35–41.

Harmon, L. J., Weir, J. T., Brock, C. D., Glor, R. E. and Challenger, W. (2008). GEIGER: Investigating evolutionary radiations. *Bioinformatics* **24**, 129–131.

Hartstone-Rose, A., Perry, J. M. G. and Morrow, C. J. (2012). Bite Force Estimation and the Fiber Architecture of Felid Masticatory Muscles. *Anat. Rec.* **295**, 1336–1351.

Hemae, K. M. (1967). Masticatory Function in the Mammals. *J. Dent. Res.* **46**, 883–893.

Henry, O., Feer, F. and Sabatier, D. (2000). Diet of the Lowland Tapir (*Tapirus terrestris* L.) in French Guiana. *Biotropica* **32**, 364.

Herbst, E. C., Lautenschlager, S., Bastiaans, D., Miedema, F. and Scheyer, T. M. (2021). Modeling tooth enamel in FEA comparisons of skulls: comparing common simplifications with biologically realistic models. *iScience* **24**, 103182.

Herrel, A., De Smet, A., Aguirre, L. F. and Aerts, P. (2008). Morphological and mechanical

determinants of bite force in bats: Do muscles matter? *J. Exp. Biol.* **211**, 86–91.

Herring, S. W. and Scapino, R. P. (1973). Physiology of feeding in miniature pigs. *J. Morphol.* **141**, 427–460.

Herring, S. W., Rafferty, K. L., Liu, Z. J. and Marshall, C. D. (2001). Jaw muscles and the skull in mammals: The biomechanics of mastication. *Comp. Biochem. Physiol. - A Mol. Integr. Physiol.* **131**, 207–219.

Holanda, E. (2006). New records of Tapirus from the late Pleistocene of southwestern Amazonia, Brazil. *Rev. Bras. Paleontol.* **9**, 193–200.

Holanda, E. C. and Ferrero, B. S. (2013). Reappraisal of the Genus *Tapirus* (Perissodactyla, Tapiridae): Systematics and Phylogenetic Affinities of the South American Tapirs. *J. Mamm. Evol.* **20**, 33–44.

Holanda, E. C., Ferigolo, J. and Ribeiro, A. M. (2011). New *Tapirus species* (Mammalia: Perissodactyla: Tapiridae) from the upper Pleistocene of Amazonia, Brazil. *J. Mammal.* **92**, 111–120.

Holmes, M. and Taylor, A. B. (2021). The influence of jaw-muscle fibre-type phenotypes on estimating maximum muscle and bite forces in primates. *Interface Focus* **11**, 1–12.

Hulbert, R. C. (2010). A new early Pleistocene tapir (Mammalia: Perissodactyla) from Florida, with a review of Blancan tapirs from the state. *Bull. Florida Museum Nat. Hist.* **49**, 67–126.

Hulbert, R. C. and Wallace, S. C. (2005). Phylogenetic analysis of Late Cenozoic Tapirus (Mammalia, Perissodactyla). *J. Vertebr. Paleontol.* **25**, 72A-72A.

Hulbert, R. C., Wallace, S. C., Klippel, W. E. and Parmalee, P. W. (2009). Cranial morphology and systematics of an extraordinary sample of the Late Neogene dwarf tapir, Tapirus polkensis (Olsen). *J. Paleontol.* **83**, 238–262.

Janzen, D. H. (1982). Seeds in tapir dung in Santa Rosa National Park, Costa Rica. *Brenesia* **19/20**, 129–135.

Ji, X.-P., Jablonski, N. G., Tong, H., Su, D. F., Ebbestad, J. O. R., Liu, C.-W. and Yu, T.-S. (2015). Tapirus yunnanensis from Shuitangba, a terminal Miocene hominoid site in Zhaotong, Yunnan Province of China. *Vertebr. Palasiat.* **53**, 177–192.

Klein, D. R. and Bay, C. (1994). Resource partitioning by mammalian herbivores in the high Arctic. *Oecologia* **97**, 439–450.

Koc, D., Dogan, A. and Bek, B. (2010). Bite force and influential factors on bite force measurements: a literature review. *Eur. J. Dent.* **4**, 223–232.

Koch, P., Hoppe, K. and SD, W. (1998). The isotopic ecology of late Pleistocene mammals in North America, Part 1: Florida. *Chem. Geol.* **152**, 119–138.

Kohn, M. J., McKay, M. P. and Knight, J. L. (2005). Dining in the Pleistocene - Who's on the menu? *Geology* **33**, 649–652.

Kuninori, T., Tomonari, H., Uehara, S., Kitashima, F., Yagi, T. and Miyawaki, S. (2014). Influence of maximum bite force on jaw movement during gummy jelly mastication. *J. Oral Rehabil.* **41**, 338–345.

Law, C. J. and Mehta, R. S. (2019). Dry versus wet and gross: Comparisons between the dry skull method and gross dissection in estimations of jaw muscle cross-sectional area and bite forces in sea otters. *J. Morphol.* **280**, 1706–1713.

Legendre, P. (2018). Package 'lmodel2.'

Leidy, T. (1860). Description of vertebrate fossils. *Post-Pliocene Foss. South Carolina (ed. Simmons, H. F.).* 99–122.

Leuthold, W. (1978). Ecological separation among browsing ungulates in Tsavo East National Park, Kenya. *Oecologia* **35**, 241–252.

Lieber, R. L. and Fridén, J. (2000). Functional and Clinical Significance of Skeletal Muscle Architecture. *Muscle Nerve* **23**, 1647–1666.

Linnaeus, C. (1758). Systema naturae ed. 10. 74.

Lizcano, D. J., Pizarro, V., Cavelier, J. and Carmona, J. (2002). Geographic distribution and population size of the mountain tapir (*Tapirus pinchaque*) in Colombia. *J. Biogeogr.* **29**, 7–15.

MacFadden, B. J. and Cerling, T. E. (1996). Mammalian herbivore communities, ancient feeding ecology, and carbon isotopes: A 10 million-year sequence from the neogene of Florida. *J. Vertebr. Paleontol.* **16**, 103–115.

MacLaren, J. A. and Nauwelaerts, S. (2016). A three-dimensional morphometric analysis of upper forelimb morphology in the enigmatic tapir (Perissodactyla: *Tapirus*) hints at subtle variations in locomotor ecology. *J. Morphol.* **277**, 1469–1485.

MacLaren, J. A. and Nauwelaerts, S. (2017). Interspecific variation in the tetradactyl manus of modern tapirs (Perissodactyla: *Tapirus*) exposed using geometric morphometrics. *J.*

Morphol. **278**, 1517–1535.

MacLaren, J. A., Hulbert, R. C., Wallace, S. C. and Nauwelaerts, S. (2018). A morphometric analysis of the forelimb in the genus Tapirus (Perissodactyla: Tapiridae) reveals influences of habitat, phylogeny and size through time and across geographical space. *Zool. J. Linn. Soc.* **184**, 499–515.

Maddison, W. P. and Maddison, D. R. (2019). Mesquite: a modular system for evolutionary analysis. Version 3.61.

Maestri, R., Patterson, B. D., Fornel, R., Monteiro, L. R. and de Freitas, T. R. O. (2016). Diet, bite force and skull morphology in the generalist rodent morphotype. *J. Evol. Biol.* **29**, 2191–2204.

Matthew, W. D. and Granger, W. (1923). New Fossil Mammals from the Pliocene of Sze-Chuan, China. *Bull. Am. Museum Nat. Hist.* **48**, 563–598.

Milewski, A. V. and Dierenfeld, E. S. (2013). Structural and functional comparison of the proboscis between tapirs and other extant and extinct vertebrates. *Integr. Zool.* **8**, 84–94.

Murie, J. (1871). The Malayan Tapir. *J. Anat. Physiol.* **6**, 131-512.19.

Nabavizadeh, A. (2016). Evolutionary Trends in the Jaw Adductor Mechanics of Ornithischian Dinosaurs. *Anat. Rec.* **299**, 271–294.

Nett, E. M., Jaglowski, B., Ravosa, L. J., Ravosa, D. D. and Ravosa, M. J. (2021). Mechanical properties of food and masticatory behavior in llamas, Llama glama. *J. Mammal.* **102**, 1375–1389.

O'Farrill, G., Galetti, M. and Campos-Arceiz, A. (2013). Frugivory and seed dispersal by tapirs: An insight on their ecological role. *Integr. Zool.* **8**, 4–17.

Olsen, S. J. (1960). Age and faunal relationships of *Tapiravus* remains from Florida. *J. Paleontol.* **34**, 164–167.

Orme, D., Freckleton, R. P., Thomas, G. H., Petzoldt, T., Fritz, S. A. and Isaac, N. (2013). CAPER: comparative analyses of phylogenetics and evolution in R. *Methods Ecol. Evol.* **3**, 145–151.

Padilla, M. and Dowler, R. C. (1994). *Tapirus terrestris*. *Mamm. Species* **481**, 1–8.

Padilla, M., Dowler, R. C. and Downer, C. C. (2010). *Tapirus pinchaque* (Perissodactyla: Tapiridae). *Mamm. Species* **42**, 166–182.

Pagel, M. (1999). Inferring the historical patterns of biological evolution. *Nature* **401**, 877–884.

Palmqvist, P., Martínez-Navarro, B., Pérez-Claros, J. A., Torregrosa, V., Figueirido, B., Jiménez-Arenas, J. M., Patrocinio Espigares, M., Ros-Montoya, S. and De Renzi, M. (2011). The giant hyena *Pachycrocuta brevirostris*: Modelling the bone-cracking behavior of an extinct carnivore. *Quat. Int.* **243**, 61–79.

Pisias, N. G. and Moore, T. C. (1981). The evolution of the Pleistocene climate: a time series approach. *Earth Planet. Sci. Lett.* **52**, 450–458.

R Core Team (2013). R: A language and environment for statistical computing. R Foundation for Statistical Computing, Vienna, Austria. Retrieved from http://www.R-project.org/.

Radinsky, L. B. (1965). Evolution of the tapiroid skeleton from *Heptodon* to *Tapirus*. *Bull. Museum Comp. Zool.* **134**, 69–106.

Radinsky, L. B. (1966). A New Genus of Early Eocene Tapiroid (Mammalia, Perissodactyla). *J. Paleontol.* **40**, 740–742.

Randau, M., Carbone, C. and Turvey, S. T. (2013). Canine Evolution in Sabretoothed Carnivores: Natural Selection or Sexual Selection? *PLoS One* **8**, 1–5.

Revell, L. J. (2012). phytools: An R package for phylogenetic comparative biology (and other things). *Methods Ecol. Evol.* **3**, 217–223.

Reynolds, P. S. (2002). How big is a giant? The importance of method in estimating body size of extinct mammals. *J. Mammal.* **83**, 321–332.

Rojas, R. R., Mora, W. V., Lozano, E. P., Herrera, E. R. T., Heymann, E. W. and Bodmer, R. (2021). Ontogenetic skull variation in an Amazonian population of lowland tapir, *Tapirus terrestris* (Mammalia : Perissodactyla) in the department of Loreto, Peru. *Acta Amaz.* **51**, 311–322.

Roulin, M. (1829). Rapport sur un Memoire de M. Roulin, ayant pour objet la decouverte d'une nouvelle espece de Tapir dans l'Amerique du Sud, fait a l'Academie royal des Sciences. *Ann. des Sci. Nat. (ed. Cuvier, M. le Baron).* **17**, 107–112.

Ruiz-García, M., Vsquez, C., Pinedo-Castro, M., Sandoval, S., Castellanos, A., Kaston, F., De, B. and Shostell, J. (2012). Phylogeography of the Mountain Tapir (*Tapirus pinchaque*) and the Central American Tapir (*Tapirus bairdii*) and the Origins of the Three Latin-American Tapirs by Means of mtCyt-B Sequences. *Curr. Top. Phylogenetics Phylogeography Terr. Aquat. Syst.*

Ruiz-García, M., Vásquez, C., Sandoval, S., Kaston, F., Luengas-Villamil, K. and Shostell, J. M. (2016a). Phylogeography and spatial structure of the lowland tapir (*Tapirus*

terrestris, Perissodactyla: Tapiridae) in South America. *Mitochondrial DNA Part A* **27**, 2334–2342.

Ruiz-García, M., Castellanos, A., Bernal, L., Pinedo, M., Kaston, F. and Shostell, J. (2016b). Mitogenomics of the mountain tapir (*Tapirus pinchaque*, Tapiridae, Perissodactyla, Mammalia) in Colombia and Ecuador: Phylogeography and insights into the origin and systematics of the South American tapirs. *Mamm. Biol.* **81**, 163–175.

Sakamoto, M., Lloyd, G. T. and Benton, M. J. (2010). Phylogenetically structured variance in felid bite force: The role of phylogeny in the evolution of biting performance. *J. Evol. Biol.* **23**, 463–478.

Sanson, G. (2006). The biomechanics of browsing and grazing. *Am. J. Bot.* **93**, 1531–1545.

Santana, S. E., Dumont, E. R. and Davis, J. L. (2010). Mechanics of bite force production and its relationship to diet in bats. *Funct. Ecol.* **24**, 776–784.

Savage, R. J. G. and Long, M. R. (1986). *Mammal Evolution: An Illustrated Guide.* UK: Facts on File Publications.

Scherler, L., Becker, D. and Berger, J. P. (2011). Tapiridae (Perissodactyla, Mammalia) of the Swiss Molasse Basin during the Oligocene-Miocene transition. *J. Vertebr. Paleontol.* **31**, 479–496.

Schindelin, J., Arganda-Carreras, I., Frise, E., Kaynig, V., Longair, M., Pietzsch, T., Preibisch, S., Rueden, C., Saalfeld, S., Schmid, B., et al. (2012). Fiji: An open-source platform for biological-image analysis. *Nat. Methods* **9**, 676–682.

Schoch, R. M. (1984). The Type Specimens of *Tapiravus validus* and ? *Tapiravus rams* (Mammalia, Perissodactyla), with a Review of the Genus, and a New Report of *Miotapirus* (*Miotapirus marslandensis* Schoch and Prins, new species) from Nebraska. *Postilla* **195**, 1–12.

Schultz, C. B., Martin, L. D. and Corner, R. G. (1975). Middle and Late Cenozoic tapirs from Nebraska Bull. Univ. Nebraska State Mus. *Bull. Univ. Nebraska State Mus.* **10**, 1–21.

Sellards, E. H. (1918). *The skull of a Pleistocene tapir including description of a new species and a note on the associated fauna and flora*. Florida. Geological survey.

Sharp, A. C. (2014). Three dimensional digital reconstruction of the jaw adductor musculature of the extinct marsupial giant *Diprotodon optatum*. *PeerJ* 1–20.

Sharp, A. C. and Rich, T. H. (2016). Cranial biomechanics, bite force and function of the

endocranial sinuses in *Diprotodon optatum*, the largest known marsupial. *J. Anat.* **228**, 984–995.

Shipley, L. A., Gross, J. E., Spalinger, D. E., Thompson Hobbs, N. and Wunder, B. A. (1994). The scaling of intake rate in mammalian herbivores. *Am. Nat.* **143**, 1055–1082.

Slater, G. J. and Van Valkenburgh, B. (2009). Allometry and performance: The evolution of skull form and function in felids. *J. Evol. Biol.* **22**, 2278–2287.

Snively, E., Fahlke, J. M. and Welsh, R. C. (2015). Bone-breaking bite force of *Basilosaurus isis* (Mammalia, Cetacea) from the Late Eocene of Egypt estimated by finite element analysis. *PLoS One* **10**, 1–23.

Szalay, F. S. (1969). Origin and Evolution of Function of the Mesonychid Condylarth Feeding Mechanism. *Evolution (N. Y).* **23**, 703–720.

Tanner, J. B., Dumont, E. R., Sakai, S. T., Lundrigan, B. L. and Holekamp, K. E. (2008). Of arcs and vaults: The biomechanics of bone-cracking in spotted hyenas (*Crocuta crocuta*). *Biol. J. Linn. Soc.* **95**, 246–255.

Therrien, F. (2005). Mandibular force profiles of extant carnivorans and implications for the feeding behaviour of extinct predators. *J. Zool.* **267**, 249–270.

Thomason, J. J. (1991). Cranial strength in relation to estimated biting forces in some mammals. *Can. J. Zool.* **69**, 2326–2333.

Thompson, C. J., Ahmed, N. I., Veen, T., Peichel, C. L., Hendry, A. P., Bolnick, D. I. and Stuart, Y. E. (2017). Many-to-one form-to-function mapping weakens parallel morphological evolution. *Evolution (N. Y).* **71**, 2738–2749.

Tseng, Z. J. and Flynn, J. J. (2015). Are cranial biomechanical simulation data linked to known diets in extant taxa? A method for applying diet-biomechanics linkage models to infer feeding capability of extinct species. *PLoS One* **10**, 1–25.

Van der Hammen, T. (1974). The Pleistocene Changes of Vegetation and Climate in Tropical South America. *J. Biogeogr.* **1**, 3–26.

Van Valkenburgh, B. (2007). Déjà vu: The evolution of feeding morphologies in the Carnivora. *Integr. Comp. Biol.* **47**, 147–163.

Vogel, E. R., Zulfa, A., Hardus, M., Wich, S. A., Dominy, N. J. and Taylor, A. B. (2014). Food mechanical properties, feeding ecology, and the mandibular morphology of wild orangutans. *J. Hum. Evol.* **75**, 110–124.

Wainwright, P. C., Alfaro, M. E., Bolnick, D. I. and Hulsey, C. D. (2005). Many-to-one mapping of form to function: A general principle in organismal design? *Integr. Comp. Biol.* **45**, 256–262.

Wortman, J. L. and Earle, C. (1893). Ancestors of the tapir from the lower Miocene of Dakota. *Bull. Am. Museum Nat. Hist.* **5**, 159–180.

Wroe, S., Crowther, M., Dortch, J. and Chong, J. (2004). The size of the largest marsupial and why it matters. *Proc. R. Soc. B Biol. Sci.* **271**, 6–9.

Wroe, S., McHenry, C. and Thomason, J. (2005). Bite club: Comparative bite force in big biting mammals and the prediction of predatory behaviour in fossil taxa. *Proc. R. Soc. B Biol. Sci.* **272**, 619–625.

Tables

Table 1: Species included in the analysis († = extinct), with the number (N) of specimens per species, age and biogeographical realm. Ages and origin were obtained from the Palaeobiology Database (Behrensmeyer and Turner, 2013).

Family	**Genus**	**Subgenus**	**Species**	**N**	**Age**	**Biogeographical realm**
Tapiridae	*Tapirus*	*Tapirella*	*bairdii* (Gill, 1865)	3	Pleist.–Holocene	Neotropical
Tapiridae	*Tapirus*	*Acrocodia*	*indicus* (Desmarest, 1819)	11	Pleist.–Holocene	Indo-Malayan
Tapiridae	*Tapirus*		*kabomani* (Cozzuol et al., 2013)	7	Pleist.–Holocene	Neotropical
Tapiridae	*Tapirus*		*terrestris* (Linnaeus, 1758)	30	Pleist.–Holocene	Neotropical
Tapiridae	*Tapirus*		*pinchaque* (Roulin, 1829)	6	Pleist.–Holocene	Neotropical
Tapiridae	*Tapirus*		*mesopotamicus* † (Ferrero and Noriega, 2007)	1	Pleistocene	Neotropical
Tapiridae	*Tapirus*		*rondoniensis* † (Holanda et al., 2011)	1	Pleistocene	Neotropical
Tapiridae	*Tapirus*	*Megatapirus*	*augustus* † (Matthew and Granger, 1923)	1	Pleistocene	Indo-Malayan
Tapiridae	*Tapirus*	*Helicotapirus*	*veroensis* † (Sellards, 1918)	2	Pleistocene	Nearctic
Tapiridae	*Tapirus*	*Helicotapirus*	*haysii* † (Leidy, 1860)	1	Plio–Pleistocene	Nearctic
Tapiridae	*Tapirus*	*Helicotapirus*	*lundeliusi* † (Hulbert, 2010)	2	Plio–Pleistocene	Nearctic
Tapiridae	*Tapirus*	*Tapiravus*	*polkensis* † (Olsen, 1960)	2	Mio.–Pliocene	Nearctic
Tapiridae	*Tapirus*		*johnsoni* † (Schultz et al., 1975)	1	Late Miocene	Nearctic
Tapiridae	*Nexuotapirus*		*marslandensis* † (Schoch, 1984)	1	Early Miocene	Nearctic
Tapiridae	*Protapirus*		*simplex* † (Wortman and Earle, 1893)	2	Oligocene	Nearctic

Table 2: Mean absolute bite force (BF) at M1 (N) and relative bite force (BF) per species +- standard deviation (SD). Bite forces are taken at the M1, near the centre of the toothrow of full adult tapirs, and are treated as maximal bite forces in this study to account for slight differences in ages between specimens. Relative bite forces were obtained by dividing the absolute bite force with the skull length.

Species	**N**	**Absolute BF M1 (N) +- SD**	**Relative BF M1 +- SD**
Protapirus simplex †	2	2289.88 +- 173.51	1.34 +- 0.16
Nexuotapirus marslandensis †	1	2228.60 +- 0.00	1.22 +- 0.00
Tapirus johnsoni †	1	3601.22 +- 0.00	1.78 +- 0.00
Tapirus polkensis †	2	3176.29 +- 1261.07	1.68 +- 0.65
Tapirus bairdii	3	5862.11 +- 1168.68	1.66 +- 0.99
Tapirus lundeliusi †	2	5136.64 +- 1009.85	1.94 +- 0.25
Tapirus veroensis †	2	5947.58 +- 987.62	2.37 +- 0.07
Tapirus haysii †	1	5943.45 +- 0.00	2.10 + 0.00
Tapirus terrestris	30	5631.49 +- 1222.35	1.75 +- 0.45
Tapirus pinchaque	6	5042.08 +- 730.51	1.84 +- 0.40
Tapirus kabomani	7	4565.72 +- 657.34	2.15 +- 0.41
Tapirus rondoniensis †	1	5798.55 +- 0.00	1.98 +- 0.00
Tapirus mesopotamicus †	1	6316.39 +- 0.00	3.07 +- 0.00
Tapirus augustus †	1	10729.41 +- 0.00	2.80 +- 0.00
Tapirus indicus	11	8609.23 +- 1770.47	2.83 +- 0.99

Table 3: Results of the one-way ANOVA and phylogenetic ANOVA for differences in relative sagittal crest height between Nearctic and Neotropical Pleistocene tapir species. Results are shown for the data with and without *T. pinchaque*. Within-group sum of squares, between-group sum of squares, F-statistic and p-values are displayed. Significant p-values are indicated in bold.

	One-way ANOVA		**Phylogenetic ANOVA**	
	Including *T. pinchaque*	**Excluding *T. pinchaque***	**Including *T. pinchaque***	**Excluding *T. pinchaque***
Within – group sum of squares	0.0033	0.0052	0.0011	0.00062
Between – group sum of squares	0.0079	0.0037	0.0033	0.0052
F	2.91	8.33	2.91	8.33
P	0.13	**0.028**	0.51	0.21

Figures

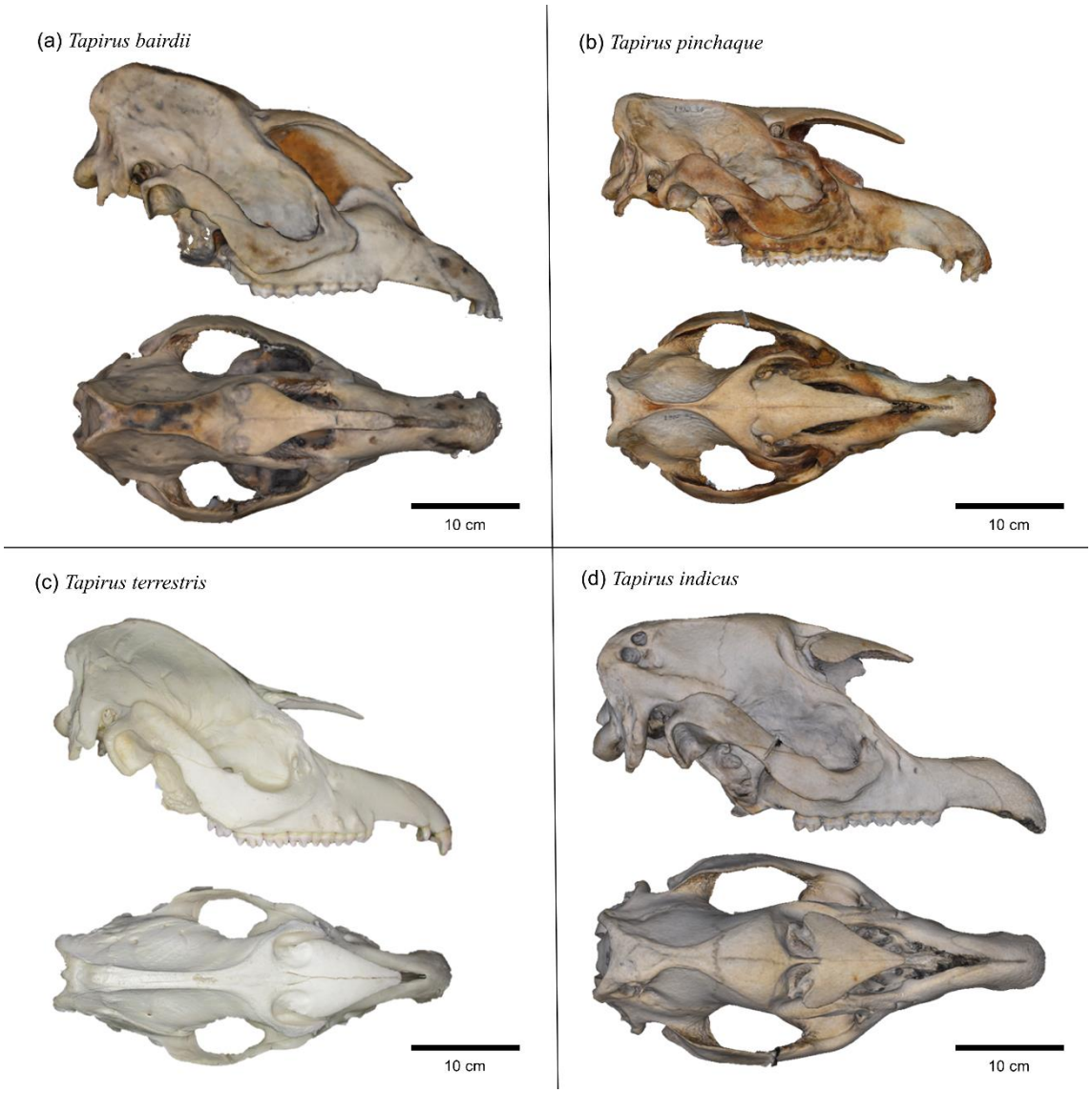

Figure 1: Skull models of extant tapirs demonstrating the variation in sagittal crest morphologies. (a) *Tapirus bairdii*. (b) *Tapirus pinchaque*. (c) *Tapirus terrestris.* (d) *Tapirus indicus*. Proportions scaled to show true size differences between the species.

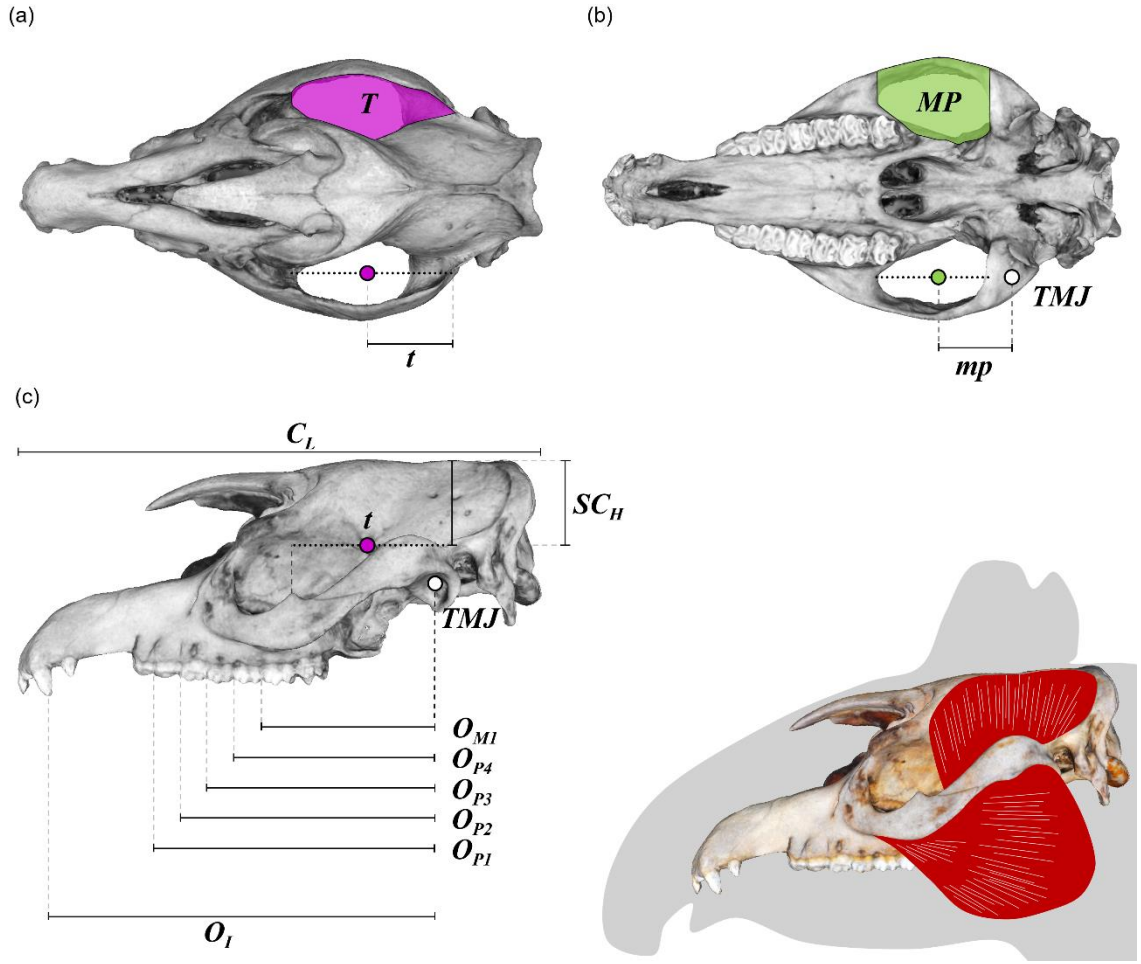

Figure 2: Diagrammatic representation of measurements recorded on images of tapir skulls for biomechanical calculations in (a) dorsal, (b) ventral and (c) lateral views. Cross sectional area and moment arm measurements for (a) *musculus temporalis* (*T, t*) and (b) *m. masseter* + *m. pterygoideus* (*MP, mp*), shown from dorsal and ventral aspects respectively. *t* and *mp* represent the distances from the centroid of the muscle group to its edge, perpendicular to the angle of muscular action. To retain consistent measuring and enable comparisons with extinct taxa, the muscle action for both muscle groups was assumed to be vertical (perpendicular to the toothrow). (c) Out-levers to the caniniform incisor (O_I) and to the teeth comprising the functional toothrow (O_{P1}, O_{P2}, O_{P3}, O_{P4}, O_{M1}) were measured from the temporomandibular joint (TMJ) to the posterior edge of the respective tooth. Total skull length (C_L) was measured from anterior premaxilla to occipital condyle; sagittal crest height (SC_H) was measured from the posterior zygomatic arch to the tallest point on the skull (with toothrow horizontal). Diagrams based on photogram of *Tapirus pinchaque* IRSNB 1186; muscular reconstruction adapted from Murie (1871).

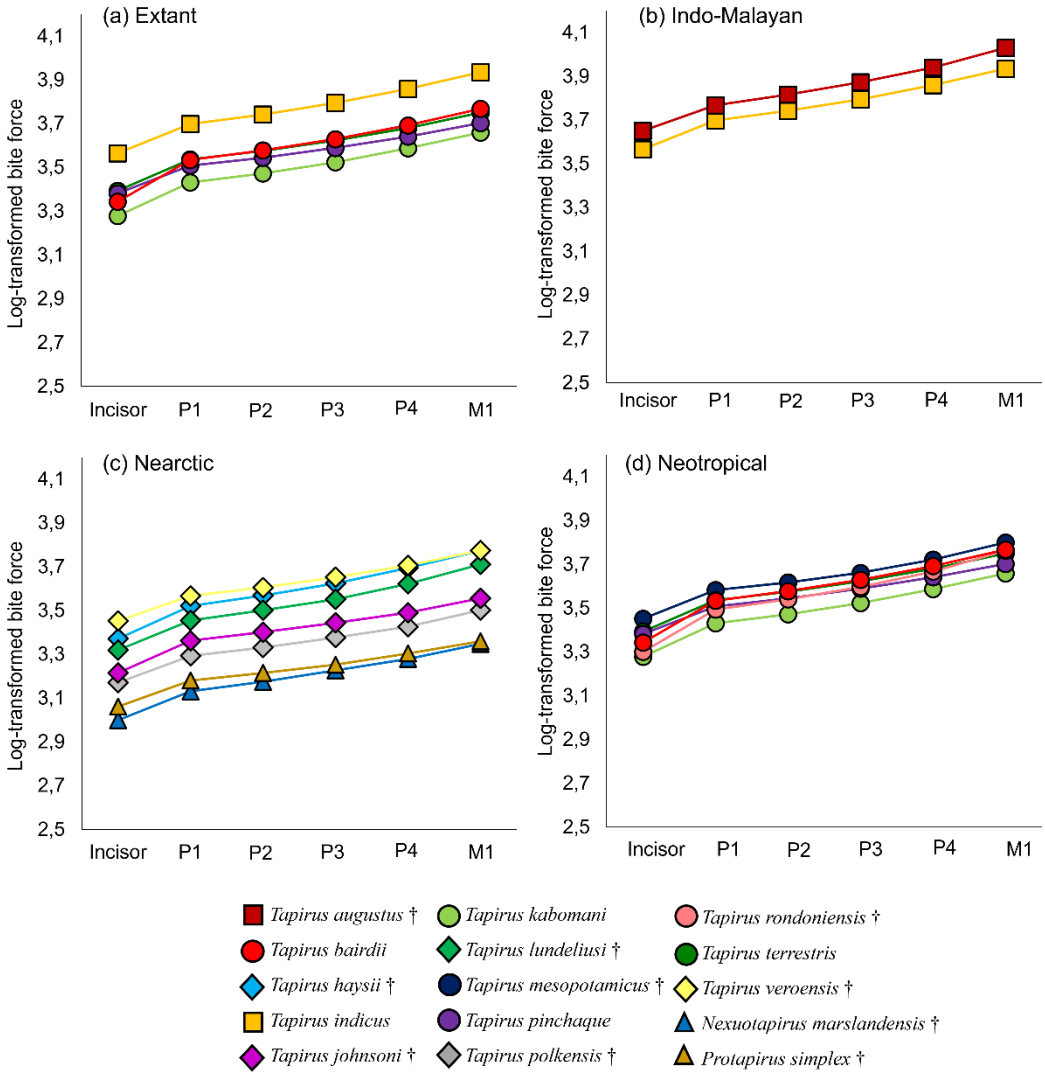

Figure 3: Tapir bite force profiles. The mean log-transformed bite forces plotted at each tooth along the skull. Bite force values are higher at the back of the toothrow. Each color represents a species. (a) Extant species. (b) Species with Indo-Malayan origin (squares). (c) Species with Nearctic origin (*Tapirus* = diamonds; non-*Tapirus* = triangles). (d) Species with Neotropical origin (circles).

Figure 4: Distribution of Pleistocene Nearctic and Neotropical tapirs (range data obtained from Palaeobiology Database, Behrensmeyer and Turner, 2013a) (hatched shading indicates overlap in geographic range between the species). For each species, a picture of the skull is provided with the chewing muscles *m. temporalis* in red and *m. masseter* in purple, together with the mean bite force (N) to demonstrate the variation in mastication morphologies and performance (see Table S1 for sources of the pictures). The difference in sagittal crest heights between Nearctic and Neotropical species is shown in the boxplot on the bottom right.

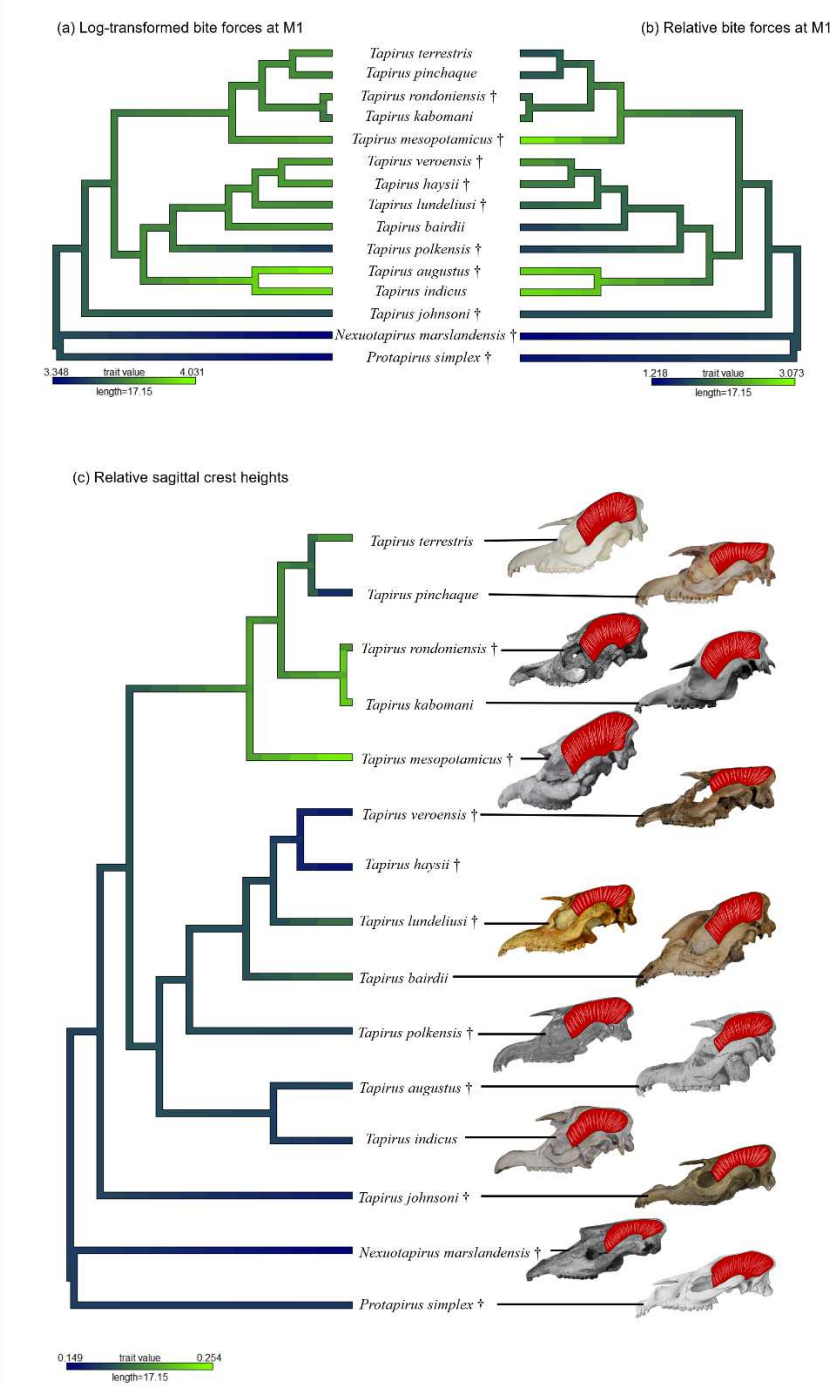

Figure 5: Tapir cranial morphofunctional traits plotted onto informal phylogeny. (a) Log-transformed bite forces at M1; (b) Relative bite forces at M1. (c) Relative sagittal crest heights. Dark tones represent low values for bite force and crest height, light tones represent high values. Generated with the R package "phytools" (Revell, 2012). For each species, a picture of the cranium is provided with the *m. temporalis* in red (with the exclusion of *T. haysii*) to demonstrate the variation in crest morphologies (see Table S1 for sources of the pictures).

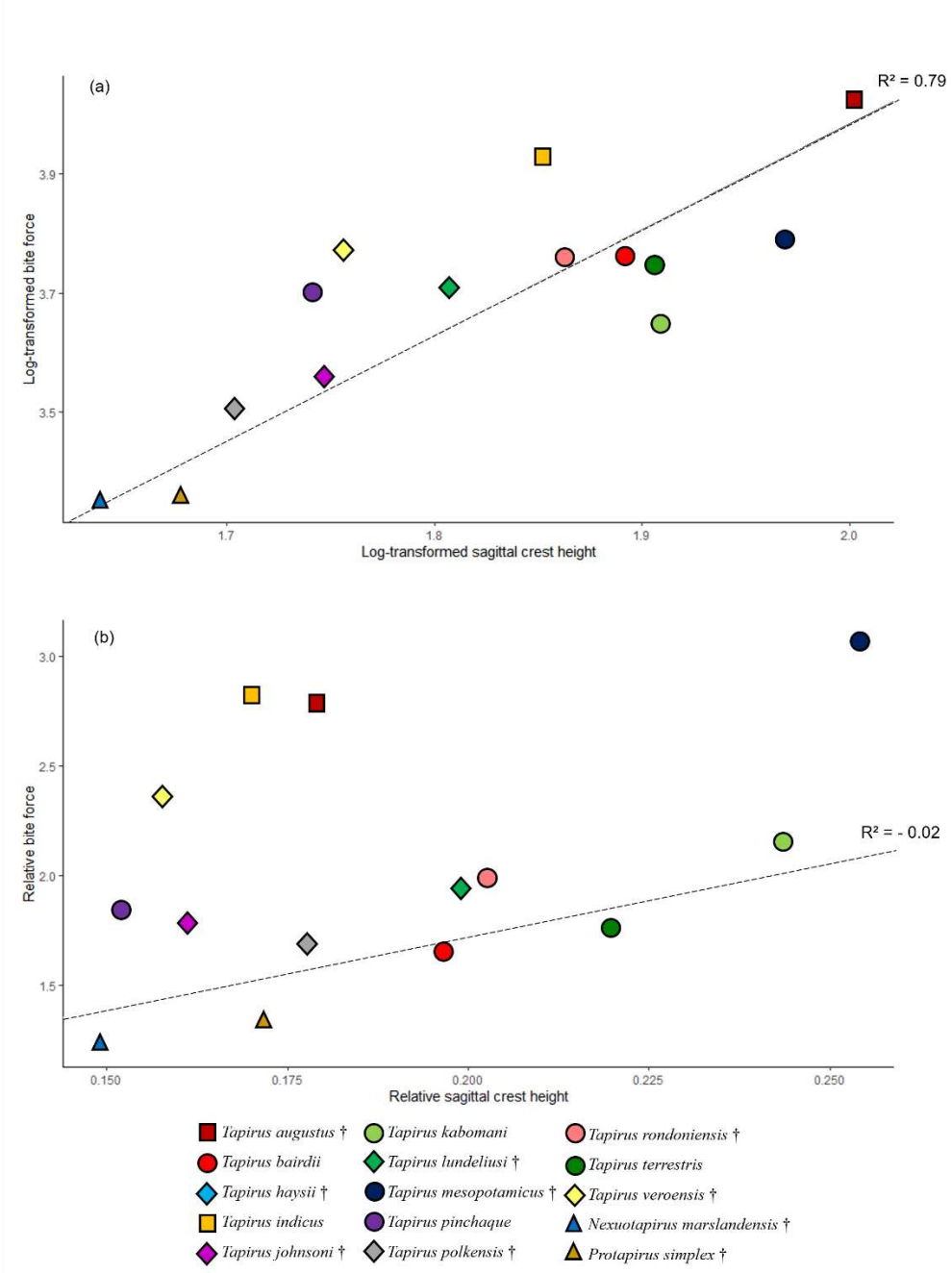

Figure 6: Phylogenetic generalised least-squares (PGLS) regression between (a) species-averaged log-transformed bite forces at M1 and log-transformed sagittal crest heights. There is a significant correlation ($\lambda = 0$, slope: 1.78 +- 0.25, $F_{(1,12)} = 50.81$, $p < 0.05$). (b) species-averaged maximum relative bite forces at M1 and relative sagittal crest heights. There is no significant correlation ($\lambda = 0.65$, slope: 3.61 +- 4.25, $F_{(1,12)} = 0.72$, $p = 0.41$). Legend: Indo-Malayan origin (squares); Nearctic origin (*Tapirus* = diamonds; non-*Tapirus* = triangles); Neotropical origin (circles).